POLITECNICO DI MILANO

School of Industrial and Information Engineering

Master Thesis in Chemical Engineering

Synthesis of cyclic oligomers of polyethylene furanoate and their purification by adsorption

Supervisor: Prof. Massimo MORBIDELLI

Co-advisors: Prof. Giuseppe STORTI

Peter FLECKENSTEIN

Author:

Loris Maestri matr. 837912

Academic Year 2015/2016

Table of Content

List of Figures

List of Tables

Abstract

Aiming to a substantial reduction of oil as a raw material for plastic market, the idea of substituting PET with PEF was proposed. PEF can be obtained by renewable sources and its performances are brilliant, thus making it a good alternative to PET. ROP was chosen as an innovative and competitive reaction pathway for PEF synthesis, requiring cyclic oligomers with high purity. In this work, cyclic oligomers of polyethylene furanoate have been produced following the cyclodepolymerization route. Reaction is promoted by high dilution using 2-methylnaphthalene as solvent, enabling the linear species to close up and form rings, the energy required was provided by heating up the system to 200 °C. In order to have a quantitative picture of the reaction, a series of calibration curves for each species was done exploiting the solvent as an internal standard. The quantitative analysis provided a feasible set of input data for mathematical modeling: it was possible to apply an equilibrium model able to predict the final equilibrium composition of cyclics and linears with very good agreement. Moreover, it was possible to estimate kinetic parameters concerning cyclodepolymerization. Solvent showed its key role, able to influence reaction yield: solvents alternative to 2-methylnaphthalene were proposed, showing interesting properties such as the possibility of running reaction at lower temperatures and increased yields. Cyclic separation was investigated briefly by using selective precipitation. Selective adsorption on zeolites at reaction conditions was proposed as a new method for the purification of cyclic linear mixtures. Using Zeolite CBV 780 in 2-MN an infinity selectivity could be observed, with the cyclics being unaffected by the adsorbent, while the Linear species showed a Langmuir type adsorption behavior. This is enabling new possibilities for combined reaction-adsorption process for the production of cyclic oligomers.

1 Introduction

In this last decade bio-based plastics have been receiving increased attention, fueled by the potential they hold to reduce emissions and to increase the security of raw material supply through the transition from fossil feedstocks to sustainable bio-based ones.

PEF is considered a bio-based alternative to the petrochemical-based plastic polyethylene terephthalate: PET. The PET bottle market amounts to about 15 mega tons which is equivalent to 5.9% of the global plastic production (the total PET production is about 50 mega tons per year and also includes fibers, films sheets and packaging) [1].

PET is produced using purified terephthalic acid (PTA) and ethylene glycol (EG): the main raw material for PTA is para-xylene which is produced by oil refining, while EG is obtained on the basis of ethylene made by oil cracking or, nowadays, also from bioethanol. By replacing the main building block of PET with FDCA, PEF is obtained: when also using renewable EG, a 100% renewable PEF can be produced.

1.1 Main aspects of replacing fossil-based PET with bio-based PEF

PET has been the dominant polymer for beverage packaging for the past decades due to its optical clarity, barrier properties and competitive performance-to-cost ratio. Even if PET has fulfilled many of the package needs, its high oxygen transmission rates together with the use of petroleum-derived building block (TA) limits its effectiveness for oxygen-sensitive beverages and environmental sustainability.

A general overview of the potential improvements in term of material's properties and environmental aspects is given below, taking into account current PET major application, the production of plastic bottles for liquid storage.

1.1.1 Comparison of physical and mechanical properties

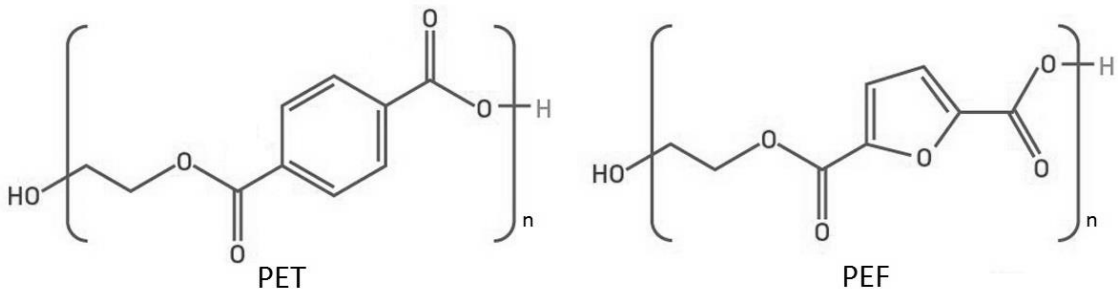

Figure 1.1.1 PET vs PEF chemical structure: the furanic ring has the same position as the benzene ring in the polymer' repeating unit.

FDCA is similar to TA but the difference in ring size, polarity and linearity results in significantly different performances. Moreover, the use of FDCA as a monomer inevitably results in a colored product, due to decarboxylation of FDCA under polycondensation reaction conditions [2]. Coloring of the final product can be avoided using 2,-5-furandicarboxylate dimethyl ester instead of FDCA itself.

Different physical, mechanical and barrier properties were explored: polyethylene furanoate showed significant improvements in terms of gas permeability and mechanical aspects making it a promising and competitive alternative to PET. Particularly PEF's O_2, H_2O and CO_2 barrier properties are superior to its oil-based analogous: permeability was measured by combined pressure-decay sorption and permeation techniques[3]–[5]. The results of these measurements are summarized in Table 1.1.1.

Table 1.1.1 Comparison of permeability values between PEF and PET

	PET	**PEF**	**Reference**
O_2 Permeability [barrer]	0.114	0.0107	[4]
CO_2 Permeability [barrer]	0.49	0.026	[5]
H_2O sorption [cm^3 STP/ cm^3 Poly*atm]	290	787	[6]
H_2O desorption [cm^3 STP/ cm^3 Poly*atm]	418	1240	[6]

To better understand those data, it is possible to introduce a Barrier Improvement Factor (BIF) defined as the permeability of a species in PET divided by the permeability of the same species in PEF. Consequently, a BIF greater than unity means a barrier improvement.

BIF evaluated with respect to oxygen and carbon dioxide are respectively ~11 and ~19, meaning that PEF exhibits 11 times lower O_2 permeability and 19 times lower CO_2 permeability than PET. This completely different PEF behavior can be attributed to reduction in chain segmental mobility resulting from a hindrance of furan ring flipping compared to the symmetrical phenyl ring in PET [7].

On the other hand, the added polarity of the furan ring in PEF imparts the increased equilibrium water solubility of ~1.8 times on average higher than PET; furthermore, PEF exhibits a significantly reduced water diffusion coefficient of ~5 times averaged with respect to PET [6].

The permeability reduction for water complements the dramatic permeability reduction for oxygen and confirms the notion that PEF can potentially serve as a viable alternative to PET in the beverage container market.

In order to replace PET on the current plastic business, also properties related to processability have to match requirements. In Table 1.1.2, the most common characteristics are compared.

Table 1.1.2 Comparison between thermal and mechanical properties of PET and PEF

	PET	PEF	Reference
Density [Kg/m^3]	1335	1428	[2]
T_g [°C]	80	87	[8]
T_m [°C]	247	211	[7]
Heat of fusion [J/g]	140	137	[8]

Processability of the final product is strongly influenced by thermal properties: heat of fusion can be considered the same, while glass transition temperature is higher and melting temperature is lower in PEF case. Higher glass transition temperature enables PEF to be successfully employed for applications in which PET cannot be used and, further, a lower melting point allows lower operating temperature during formation processes like extrusion or injection molding.

1.1.2 Energy consumption and Greenhouse gas (GHG) emissions

In this subsection a comparison between the processes involved in production of PET and PEF is shown starting from the initial raw material, following a classical polycondensation reaction pathway.

Production of PET starts with the oxidation of p-xylene with air into terephthalic acid which is then polymerized with EG. The alternative process using FDCA is similar: 5-HMF and HMF ethers are oxidized with air into FDCA and subsequently polymerized with EG to form PEF. In the case of PEF synthesis, the oxidation step operates at lower temperatures (180 ˚C *vs.* 210 ˚C) and pressures (7 bar *vs.* 12 bar) than their petrochemical counterparts [1].

Considering fructose as raw material from which obtaining FDCA and the operating conditions of 220 ˚C and 50 bar [1], the NREU (non-renewable energy use) and GHG (greenhouse gasses) values per ton of product are reported in the Table 1.1.3.

Table 1.1.3 Results of the environmental impact analysis for the system "cradle to grave"

	NREU [GJ/ton]	GHG [CO_2 eq/ton]	Reference
PEF	33.8	2.05	[1]
PET	69.4	4.44	[1]
Reduction PEF vs. PET	51%	54%	[1]

Based on global PET bottle market (approximatively 15 Mt per years, one-third of the global PET production) complete replacement of PET by PEF would result in savings of 520 PJ for NREU and 35 Mt of CO_2 eq. respectively.

1.2 Plant based monomer for PEF production: 2, 5- furandicarboxylic acid

2, 5- furandicarboxylic acid (FDCA) belongs to the class of molecules known as furanics, which have been referred to as "Sleeping Giants" because of their enormous market potential. The US Department of Energy placed those molecules in the top 12 of high-potential bio based products [9]. They were never commercialized due to the high cost of production especially for the synthesis of 5-hydroxymethyl furfural (5-HMF) a strategic intermediate for production of different chemicals. The main barrier to commercial production of 5-HMF is that it is not stable under the acidic conditions needed for its formation and that it further reacts to form levulinic acid (LA) and formic acid (FA)[10].

5-HMF can be seen as a strategic key intermediate for the transition from fossil-based industrial chemistry to bio based industrial chemistry.

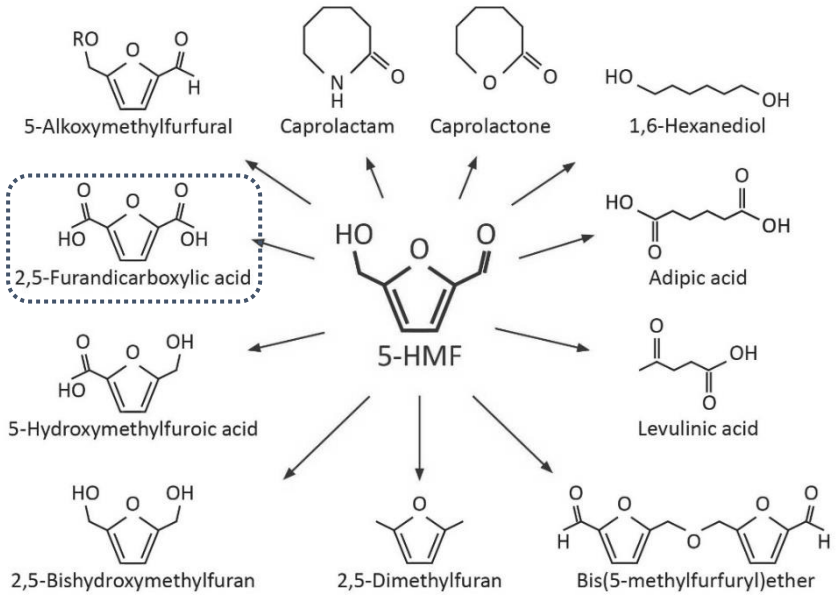

Figure 1.2.1 5-HMF as a strategic intermediate chemical for replacing fossil-based chemical compounds

FDCA molecule was discovered by Fittig and Heinzelmann in 1876 and in 1946, Celanese Corporation of America firstly patented PEF production starting from FDCA. Only five years later, an U.S. patent concerning PEF synthesis was released.

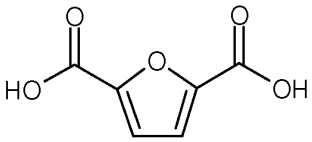

Figure 1.2.2 Chemical structure of 2,5-furandicarboxylic acid (FDCA)

However, researches both on FDCA and consequently PEF synthesis and production were left apart until the second half of the 19th century, when many authors discovered efficient and cheaper ways of producing 5-HMF from fructose and other sugars[11]–[13].

Those improvements allowed potential FDCA large-scale production, giving again power to FDCA polymer based researches.

Two different pathways for FDCA synthesis were explored: the first involving dehydration of hexose derivatives with the drawbacks of long reaction time and low yield [14] and the second, more promising, exploiting the selective oxidation of 5-HMF.

Both reactions are still an important topic in research, trying to find the best catalyst between different noble metals in order to promote FDCA production shortening reaction time[15], [16].

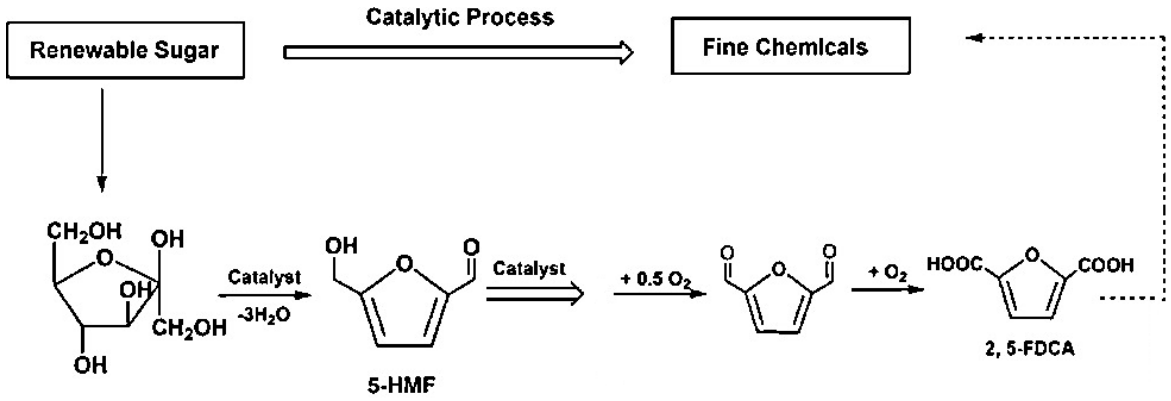

Figure 1.2.3 Example of a process aimed to produce fine chemicals starting from renewable sources: conversion of sugars into 5-HMF and FDCA and subsequently into chemicals for different usages.

1.3 PEF synthesis

Research on PEF synthesis is still on going, so all the conventional polymerization techniques are potentially applicable. Since actually PET is mainly produced by direct polycondensation reaction [1], [17], this reaction will be firstly discussed; the possibility of using Ring Opening Polymerization will be explained later.

1.3.1 Traditional polycondensation

Synthesis of PEF can follow different pathways. The similarity between the monomer FDCA and TA suggests polycondensation as a possible route. Many authors successfully synthetized and characterized the final product following this technique [2], [7], [17]–[20]. In Figure 1.3.1 the involved reaction is shown.

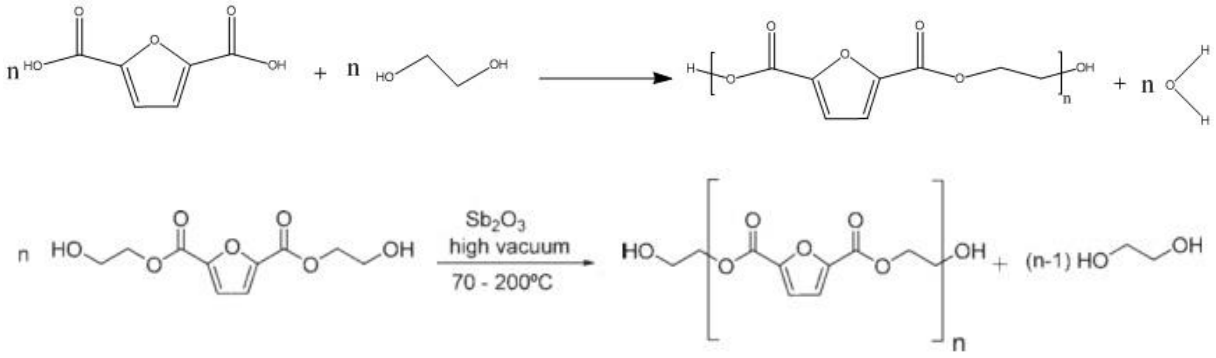

Figure 1.3.1 PEF polycondensation starting from FDCA and EG-ended FDCA [18]

Both starting with FDCA or EG-ended FDCA, polycondensation reaction involves formation of a byproduct, which is limiting the final yield. Removal of the byproducts dramatically afflicts the whole process rate, ending up with long reaction time (hours to days) to achieve sufficiently high molecular weight. This aspect become especially problematic when the viscosity of the mixture increases, thus when chain propagation is occurring. Due to this problem, a solid-state post polymerization is often applied to increase the molecular weight of the final product. Exploiting this approach, the final PEF will not be able to compete its fossil-based opponent since the final PET price is strictly related to oil-price that in these years is at its minimum. It is believed that in future the biomass-price will be lower than its actual price, thus giving the possibility to FDCA to compete with TA [2].

1.3.2 Ring Opening Polymerization (ROP)

Overcoming byproduct formation is possible by Ring Opening Polymerization, a technique which involves reaction of monomers in form of cycles leading to the final polymer without any byproducts evolution.

The global process thus includes two steps: synthesis of a tailored cyclic monomer and subsequent opening to the final polymer, as shown in Figure 1.3.2.

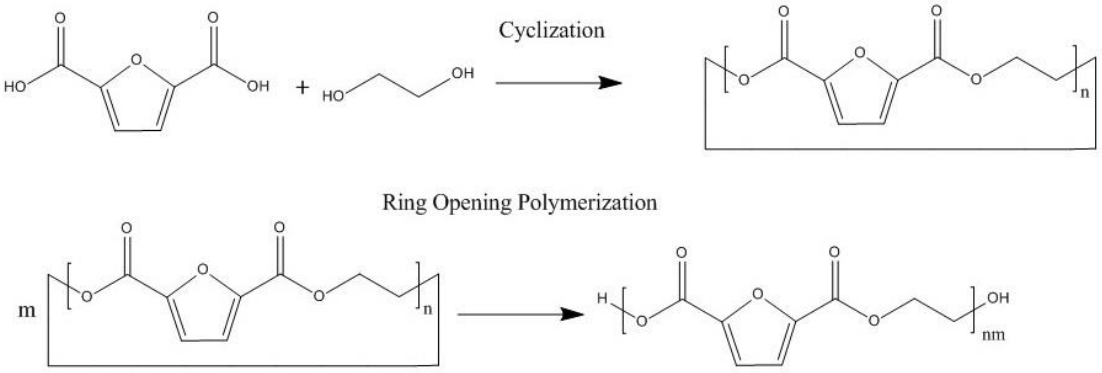

Figure 1.3.2 Global reaction scheme: cyclic monomer synthesis and ROP

ROP is performed using those tailored monomers with the assistance of different catalysts [21], [22]. Ring opening is a chain polymerization consisting of a series of initiations, propagation and termination steps in which monomers are attached to the growing chain in propagation. Unlike step polymerization, monomer does not react with monomer and larger- sized species do not generally react with each other in ROP. Many ring-opening polymerizations proceed as living polymerizations: polymer molecular weight increases linearly with conversion and the ratio of monomer to initiator[23].

Up to now a variety of cyclic monomers have been successfully polymerized by ring opening process but, practically, widespread application of ROP is hindered by the limited efficiencies for synthesizing and isolating many types of cyclic oligo esters[21]. Thus, an efficient production of cyclic monomer is crucial to match the requirements of ROP.

1.3.3 Advantages of ROP

The advantages directly related to ROP are several, promoting it as a very performing and strategic way of producing high molecular weight polymers.

First of all, ROP using the appropriate initiators affords rapid reactions (2-6 min) without measurable heat release [24], thus allowing an overall higher productivity. Using ROP, low-molecular-weight species are converted to high-molecular-weight products without formation of byproducts because cyclic oligomers would not contain end groups; in the case of PEF, the main one is water that is a direct consequence of polycondensation reaction. Final molecular weights are more predictable, and polymer has lower polydispersity index[25], meaning a better control of the process. Another important aspect is that this kind of approach allows a variety of fabrication techniques not possible with viscous high-molecular weight polymers: conversion of monomers to cyclic oligomers permits simultaneous processing and polymerization directly in the desired product shape. This is due to the fact that the mixtures of cyclic oligomers have melting points significantly lower than individual ring sizes, and have very low viscosity in the melt (viscosity is similar to the solvent's one).

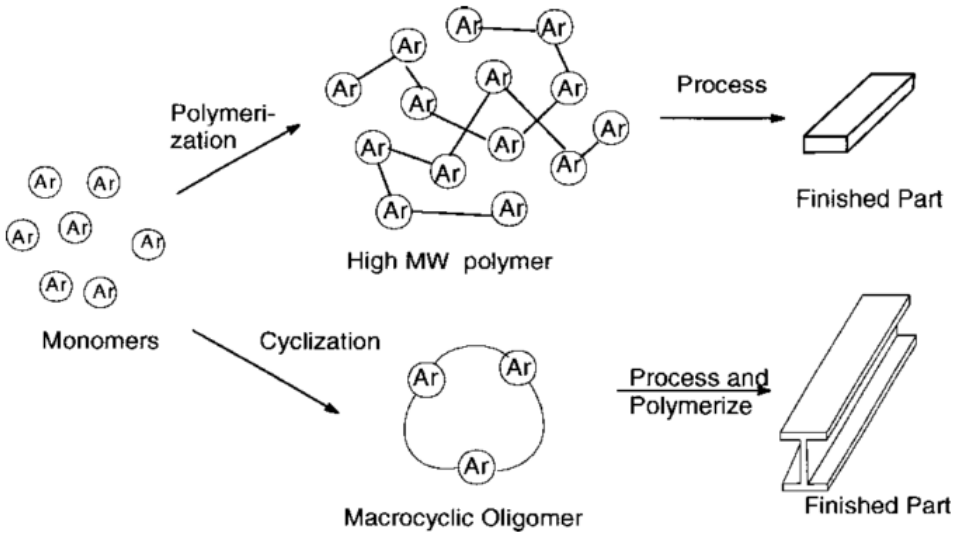

Figure 1.3.3 Example of simultaneous processing and polymerization: low viscous mixture of cyclic monomers can be directly injected in a preformed mold and directly polymerized to the final finished part [24].

1.4 Synthesis of cyclic oligomers of ethylene furanoate (CyOEF)

Once identified ROP as a strategic reaction path, two major problems needed to be solved: cyclic monomers with high purity and yield are required. The intermediate synthesis of cyclic oligomers can be considered as the rate-determining step of the process, thus different routes were explored according to literature [22], [26]–[29].

Cyclization reaction, how a linear molecule close to form a cycle, is first explained and then different routes of reaction are shown.

1.4.1 Cyclization *vs.* Linear Polymerization

Cyclization reaction is a competitive reaction taking place in standard step polymerization; the extent to which cyclization occurs during polymerization depends on whether the polymerization proceeds under equilibrium control or kinetic control, the ring sizes of the possible cyclic products, and the specific reaction conditions.

Thermodynamic stability decreases with increasing strain in the ring structure, which is of two types: angle strain and conformational strain. Ring structures of less than five atoms are highly strained due to the high degree of angle strain, that is, the large distortion of their bond angles from the normal tetrahedral bond angle. Bond angle distortion is virtually absent in rings of five or more members. For rings larger than five atoms the strain due to bond angle distortion would be excessive for planar rings. For this reason, rings larger than five atoms exist in more stable, nonplanar (puckered) forms.

Kinetic feasibility for the cyclization reaction depends on the probability of having the functional end groups of the reactant molecules approaching each other. The probability of ring formation decreases as the probability of the two functional groups encountering each other decreases. The effect is reflected in an increasingly unfavorable entropy of activation.

The overall ease of cyclization is thus dependent on the interplay of two factors: the continuous decrease in kinetic feasibility with ring size, and thermodynamic stability.

Figure 1.4.1 Example of ring chain equilibrium: a long linear chain is in equilibrium with its cyclic configuration together with the smaller linear part of it.

Low concentrations of monomers favor cyclization since it is a unimolecular (intramolecular) reaction, while linear polymerization is a bimolecular (intermolecular) reaction.

Cyclization can follow different mechanisms:

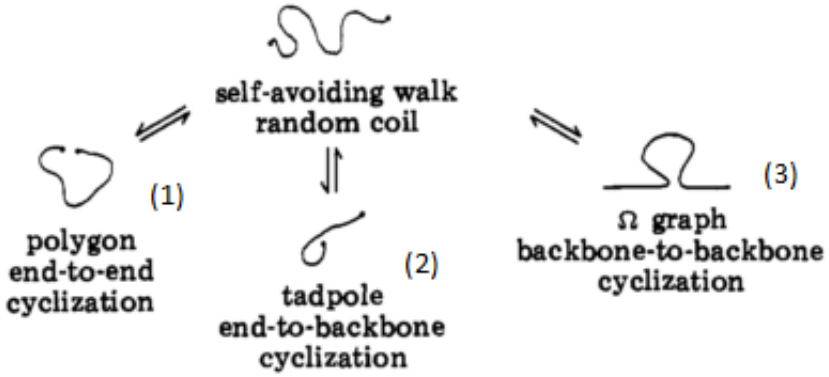

Figure 1.4.2 Main cyclization mechanisms happening on a linear chain enabling ring closure [30]

Case (1) is the *tail biting reaction* in which the two active ends of a chain react closing the chain on itself. Case (2) is instead *backbiting*, which involves an intramolecular (interchange) nucleophilic substitution reaction, in case of cyOEF, the attack of the hydroxyl end group on one of its ester carbonyl groups. Case (3) is the Ω *biting reaction* typical of ester groups in a particular position along the chain that interacts whit another one to perform cyclization. Cyclics are formed mainly by backbiting reactions along the chain [31].

For the production of cyOEF three methods were studied and applied for cyOEF [32]–[34], as briefly summarized in the following.

1.4.2 Pseudo-high dilution method

Pseudo-high dilution concept was firstly applied by D.J. Brunelle for PBT [35], but was later adapted for PEF by Pfister et al. [36] and Morales and Huerta [37] . Furandicarboxylic chloride FDCC is synthetized starting from FDCA and thionyl chloride $SOCl_2$ with simultaneous removal of hydrochloric acid, as shown in Figure 1.4.3.

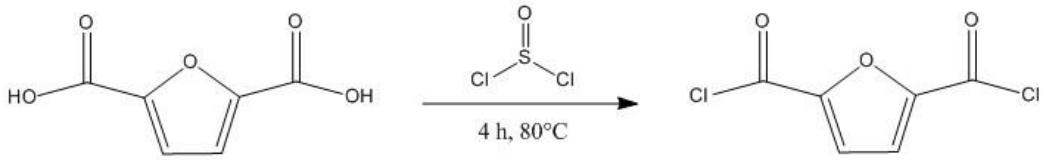

Figure 1.4.3 Synthesis of FDCC starting from FDCA and thionyl chloride at low temperature

This method involves as an additional step the reaction between FDCC and ethylene glycol under pseudo-high dilution. The reaction was run using dichloromethane as solvent and 1,4-diazabicyclo [2.2.2] octane (DABCO) as catalyst: an equimolar flow of THF-dissolved FDCC and EG were injected at very low flow rates into a large reaction volume.

This way intermolecular cyclization reaction is promoted and chain growth reaction is, on the contrary, minimized because kinetics proceeds faster than addition rate giving to the molecules the possibility to react.

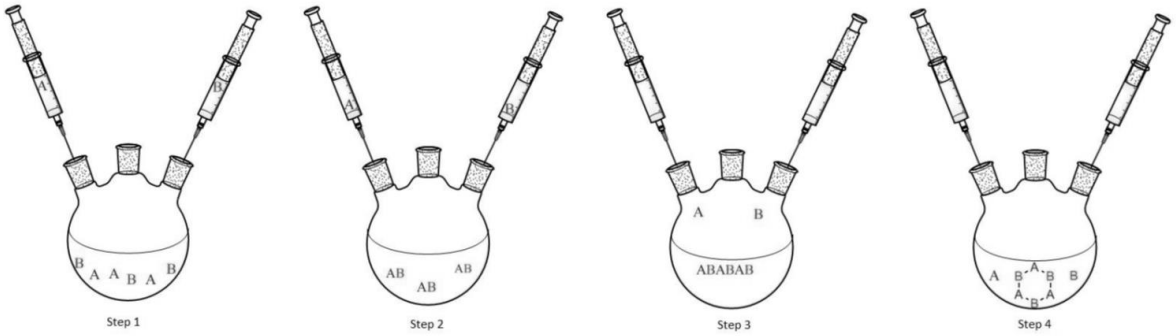

Figure 1.4.4 Scheme of a pseudo high-dilution system. The monomers start being fed into the flask (1); the reagents start reacting while new monomers are still slowly fed (2); longer chains are formed and before the newly fed monomers react to form longer polymers (3), cyclic species are formed (4).[32]

The interesting features of this reaction route is the possibility of synthetizing the intermediate cyOEF at low temperature (0°C) or ambient and therefore low thermal energy consumption. Unfortunately, drawbacks are severe: FDCC synthesis has, as byproducts, HCl and SO_2 that are toxic, corrosive and not environmental friendly chemicals. This is unsuitable for a process

intended to be “green”. Moreover, the yield is typically in the range of 60% with the additional problem, that the side products are not recyclable. All these problems together with the complexity related to the multi-solvent and multi-catalysts system have made this process not suitable for a scale up.

1.4.3 Reactive distillation

In 2000 Robert R. Burch proposed another cyclization approach consisting in reactive distillation for the formation of cyclic polyethylene isophthalate [21], which was applied to the production of cyOEF [34]. The driving force in this case is the removal of a species to shift the equilibrium towards cyclic products. In case of cyclic oligomers of ethylene furanoate, dimethyl furandicarboxylic acid (me-FDCA) is charged in a reactor together with an excess of ethylene glycol and converted to short hydroxyl-end group linear chains in the presence of a catalyst. Those linear chains are then diluted in DCB and the solution is distilled.

During distillation, the excess of EG is stripped thus reducing the EG/FDCA ratio towards unity, corresponding to cycles formation. Reactions involved in this method are shown in Figure 1.4.5.

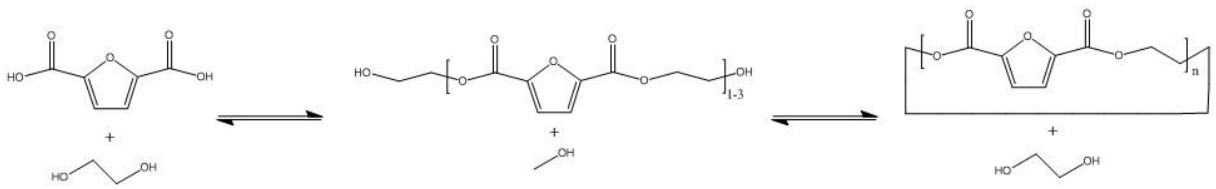

Figure 1.4.5 Reaction scheme of reactive distillation: initial polymerization step involving FDCA and EG, subsequent MeOH release and final ring closure.

The first attractive improvement of this method is represented by the high yield achievable, which is up to ~85%. Furthermore, the unreacted species can be recycled as a raw material. A major limitation concerns the impact of water, which promote hydrolysis of the products hence drastically reducing the final yield: the reaction must be run under dry conditions, even avoiding contact with air. Also from the energy point of view, this method is more energy intensive since the solvent has to be heated up until its boiling point (DCB ~200°C).

1.4.4 Cyclodepolymerization reaction

Cyclodepolymerization is the reaction focus of this work. The name of the reaction itself explains the mechanism behind: long polymer chains are converted back to shorter chains and cyclic species. Research is still on going on this topic in order to let become this route a reliable tool for cyclic production [31], [38]–[40]. Kamau et al. successfully applied this method to convert PET to their cyclic equivalent with high yield (94%) [39].

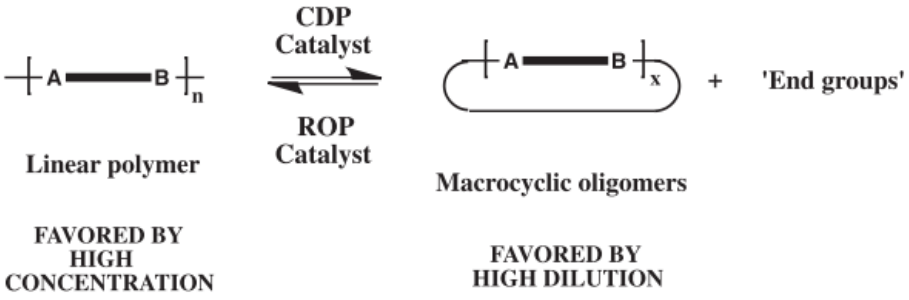

Figure 1.4.6 Cyclodepolymerization reaction and backward ROP reaction to high molecular weight linear polymers [40]

The synthesis of the cyclic monomer is carried out in two steps: FDCA and EG are put together to give short chains oligomers ($n < 10$) and subsequently converted into cyclic molecules under high dilution, the second reaction is limited by thermodynamic equilibrium. This reaction was already studied with good results[33].

The reaction was run with stannoxane as a catalyst. An alternative catalyst can be dibutyltin oxide, that can be especially convenient because it is the same catalyst exploited for prepolymer synthesis thus already available in the process. Dibutyltin oxide is a catalyst largely employed for ROP [22], [31], [39], thus is suitable also for the reverse reaction.

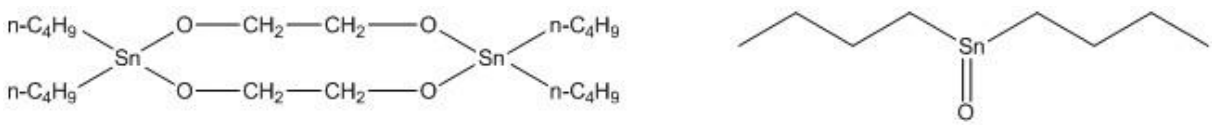

Figure 1.4.7 Chemical structure of stannoxane (left) and dibutyltin oxide (right)

The absence of a catalyst would have a positive impact on the final saleable product, since nowadays studies are ongoing on possible food contamination by heavy metals that diffuse

from the plastic packaging to food (especially liquids)[41]. In the specific case of organotin compounds, metals have shown neuro-toxic effects in animals and cytotoxic effects in humans and animals and can affect sex differentiation, resulting in masculinization of females or infertility in male aquatic animals[42].

Nevertheless, the reliability of the reaction will be deepened and its yield quantified in this thesis.

High dilution is the key point of this reaction, as explained in paragraph 1.4.1, in particular in order to obtain high yields is required a concentration less than 3%w/v [40]. During reaction, different-sized species are formed with the dominant dimer presence [23].

This cyclization route is able to produce cycles with high yield in relatively short time (1-3 h) and also in this case it is possible to precipitate out cyclic species. Once recovered the solid cyclic product, the linear unreacted species can be recycled in a new reaction. Temperature involved are high to help dissolution of the crude material and to guarantee relatively fast kinetics but respect to reactive distillation no heat of vaporization is involved, ending up with a less energy-intensive process.

Drawbacks in this case concern the preliminary synthesis of pre-PEF via polycondensation under vacuum and the high dilution conditions needed to close linear chains. With the idea of scaling up this process, high dilution can be a problem since reactors must be big enough to contain the solvent needed for a reasonable production. On the other hand, pre-PEF synthesis can be integrated in the process with the actual technology applied for melt polycondensation, able to deal with high viscosity slurries.

Solvents are widely recognized to be of great environmental concern. The appropriate selection of the solvent for a process can greatly improve the sustainability of a chemical production process. In chemical industry, solvents are used in the production of chemicals as media for reactions as well as for separation/purification. In recent years a lot of efforts have been spent on green chemistry, trying to be as much sustainable as possible; nowadays is available the so called “green metrics” [43] used to evaluate the sustainability of an entire process. Selection guide are already available on literature [44].

Solvents can strongly afflict process performances [45] especially in cyclodepolymerization reaction [46], [47]; introducing non trivial problems to overcome.

Therefore is necessary to find a suitable solvent for both the cyclodepolymerization reaction and the subsequent purification of the final product: in order to guarantee the usage of the same solvent for different process steps.

1.4.5 Cyclization reaction via heterogeneous catalysis

A relatively new method for cyclic production involving heterogeneous catalysis deserves attention. Si-gel is functionalized with titanium isopropoxide providing an anchoring on the surface on which a linear chain can attach [48].

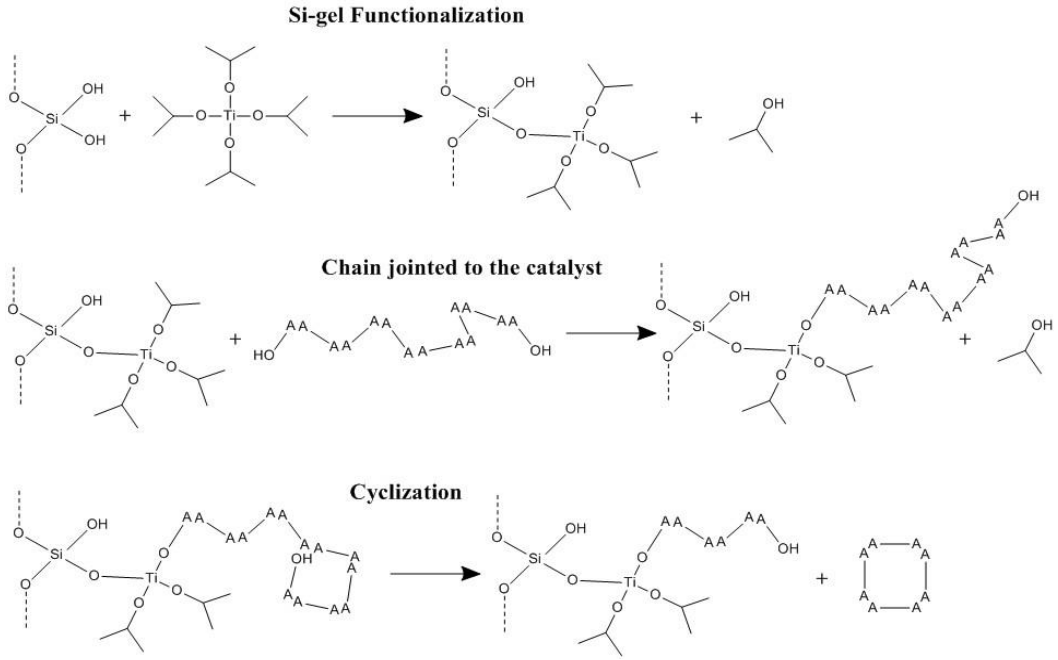

Figure 1.4.8 Functionalization of Si-gel particles with titanium isopropoxide, linkage of the chain on the catalyst and final cyclization reaction

The reduction of their mobility force them to close up as a cycle: cyclization in this case can be justified by the increased probability of an end group to get in contact to the chain. For simplicity, the linear chain of FDCA EG is represented as A. Isopropanol is distilled out during reaction. The advantages of this reaction route is the efficiency in cyclic production, giving almost pure cycles with moderate yield. The unreacted product can be recycled together with silica-gel.

1.5 Purification

Production of PEF via ROP requires, together with high cyclic oligomers yield, high purity of the raw material. The presence of linear species can affect the final conversion, limiting the achievable polymer molecular weight, its polydispersity and consequently its final properties such as melting behavior, melting and glass transition temperatures. Purification of the final product is, therefore, crucial.

The typical methods applied on a lab scale consists in coupling precipitation and purification via Si-gel column adsorption.

Precipitation of cyclic products exploits the different solubility of the single cyclic species: cooling the reaction mixture, only cyclic species are recovered. The purity of the final product is in the order of 80-85%, but aiming to a cyOEF purity ≥ 98% a further purification step is necessary. For this reason, Si-gel adsorption is used to selectively remove polar chains from the mixture.

Even if, in principle, this method can provide good purity, several drawbacks are limiting its use. The first drawback concerns the purity achievable with precipitation: roughly, 15% of the cyOEF are withhold in the reacting mixture. The second disadvantage is the solvent exchange needed for Si-gel adsorption: in fact, a solvent able to dissolve both linear and cyclic species is needed. Thinking of a continuous process, keeping the same solvent for both reaction and purification would be desirable.

1.5.1 Adsorption on zeolites

Zeolites are materials already exploited for purification purposes[49], [50]: their particular structure acts as a molecular sieve able to trap specific components.

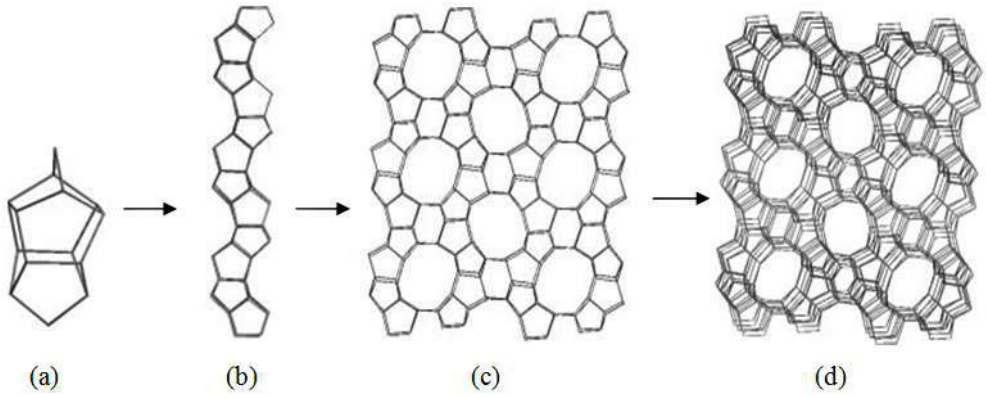

Figure 1.5.1 Example of a typical zeolite structure: (a) the pentasil unit; (b) chains of pentasil units; (c) layers of these chains; and (d) layers linked across inversion centers [51]

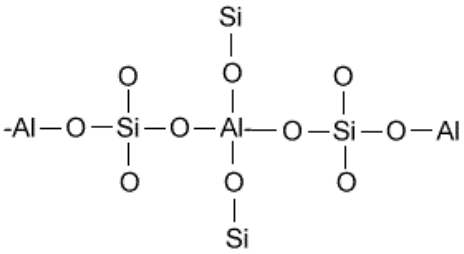

Figure 1.5.2 Basic Zeolite Structure

Structurally the zeolites are 'framework' aluminosilicates, which are based on an infinitely extending three-dimensional network of AIO4 and SiO4 tetrahedral linked to each other by sharing all of the oxygens. Zeolites may be represented by the empirical formula:

$$M_{2/n}O{\bullet}Al_2O_3{\bullet}xSiO_2{\bullet}y\ H_2O$$

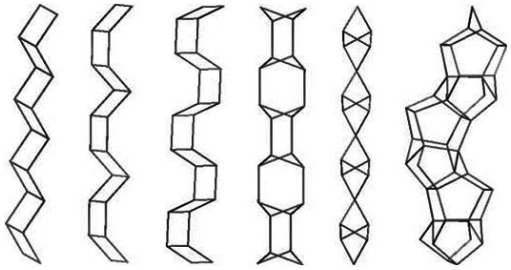

Figure 1.5.3 Different chains due to different starting units [54]

In this oxide formula, *x* is generally equal to or greater than 2 since AlO_4 tetrahedral are joined only to SiO_4 tetrahedral, *n* is the cation valence. The framework contains channels and interconnected voids that are occupied by the cation and water molecules [52]. The possibility of tuning zeolites structures allows their usage as purification medium for molecules with different sizes or shapes[53]–[55]. A clarifying example is Molex™ process [49], [50] applied in petrochemical fields, in which mixture of branched, linear and cyclic hydrocarbons of different sizes are separated through selective adsorption on zeolites.

Since the final product of a cyclodepolymerization reaction consist in a mixture of linear and cyclic oligomers of different sizes, the same approach can be exploited for purification step.

1.6 Aim of this work

This work aims at full characterization of cyclodepolymerization reaction, which is needed to apply this reaction route as a feasible method for the cyclic monomer production used for subsequent ring opening polymerization. A quantitative analysis tool is therefore needed to obtain reliable data. With the data collected a suitable mathematical model will be developed, which can be used as a tool for process modeling. Last aspect of the synthetic part is the screening of different solvents suitable for cyclodepolymerization to understand the impact of the solvent on the final yield and furthermore, to give a more environmental sustainable imprint to the process.

The second aim concerns the purification of the final product: different purification methods will be explored and characterized; moreover, since the project is in close contact with an ongoing scale up of cyclodepolymerization using 2-methylnaphthalene as solvent, purification experiments will be carried out mainly in this solvent to find a useful method for purification at conditions of pratical interest.

2 Experimental Procedures

2.1 Materials and Instrumentations

2.1.1 Materials

2,5-furandicarboxylic acid dimethyl ester (Me-FDCA) was purchased from **CM Fine Chemicals.** Dichloromethane (DCM) (99.99%, HPLC grade), diethyl ether (Et_2O)(≥ 99.8%, BHT inhibitor), acetonitrile (≥ 99.9%, HPLC grade), ethylene glycol (EG) (anhydrous, 99.8%), dichlorobenzene (DCB) (99%) and titanium isopropoxide (TTIP) (99.999%), were purchased by **Sigma Aldrich**. n-Hexane (≥ 98.0%), 2-methylnaphthalene (2-MN) (≥ 95.0%), dibutyltin oxide (Bu_2SnO) (≥ 98%), methanol (≥ 99.9%), acetone (≥ 99.5%) were purchased from **Merck**. Tetraethylene glycol dimethyl ether (T-glyme) (99%) and diphenyl ether (PhE) (99%) were purchased from **ACROS.** Chloroform (0.006% water, stabilized Amylene), trifluoroacetic acid (TFA) and isopropanol (99.95%, HPLC grade) were purchased from **Fisher Chemical**. Dimethyl Sulfoxide (DMSO) (>99.8%) and Si-gel high purity grade (w/Ca, ~0.1%) (Pore size 60Å, 230-400 mesh particle size) was purchased from **FLUKA**. Zeolite CBV 780 was purchased from **Zeolyst International**. Zeolites HSZ-390HUA, HSZ-890HUA, HSZ-980HUA were purchased from **Tosoh Corporation**. Millipore water was purified using **Synergy Ultrapure Water System**. All chemicals were used without any further purification.

2.1.2 Instrumentations

High performance liquid chromatography (HPLC) was performed on an Agilent 1100 series HPLC system with quaternary pump, auto sampler and UV detector using a ZORBAX Eclipse XDB C18 column, 150×4.6 mm (pore size 5 µm and surface area 180 m^2/g) from Agilent. Eluents used were acetonitrile and Millipore water both stabilized by 0.1 v/v% trifluoroacetic acid with a total flow-rate of 1 mL/min and elution volume of 60 mL per sample. Samples were dissolved in HFIP/$CHCl_3$ (15% vol HFIP) and 10 mL were injected per analysis. UV detection was performed at 280 nm wavelength.

Gel Permeation Chromatography (GPC) was performed on an Agilent 1200 series HPLC system with quaternary pump and automatic injector. GPC/SEC columns including 4× ResiPore, 300×7.5 mm (molecular range up to 550,000, column efficiency > 80,000 p/m) and ResiPore Guard column were purchased from Agilent. The eluent used was chloroform. Samples were dissolved in HFIP/$CHCl_3$ (15% vol HFIP) and 10 mL were injected per analysis.

2.2 Mass Calibration Curves of HPLC

A solution of known mass concentration of 2-MN in GPC solvent was prepared according to Table 2.8.1. This solution was subsequently diluted into six different vials leading to six different solutions with known concentration. Each vial was stored in the fridge until the beginning of the analysis to avoid, as much as possible, solvent's evaporation. The solutions were then injected to HPLC and the UV peak area correlated with the concentration were obtained. This was repeated to obtain calibration curves for DCB, diphenyl ether, prepolymer, pure 2-membered OEF and a mixture of purified cyclic oligomers.

2.3 Reactions

2.3.1 Synthesis of pre-polymer by melt polymerization of me-FDCA and EG

A 250 mL three-neck round bottom glass reactor was equipped with magnetic stirrer, reflux condenser, Liebig condenser and a small round bottom collection flask connected to the cooler through a drip tip of take-off adapter. Through the adapter, the experimental setup was jointed to a Schlenk line with manifolds directly connected to vacuum pump and to nitrogen source. The figure below shows this experimental setup.

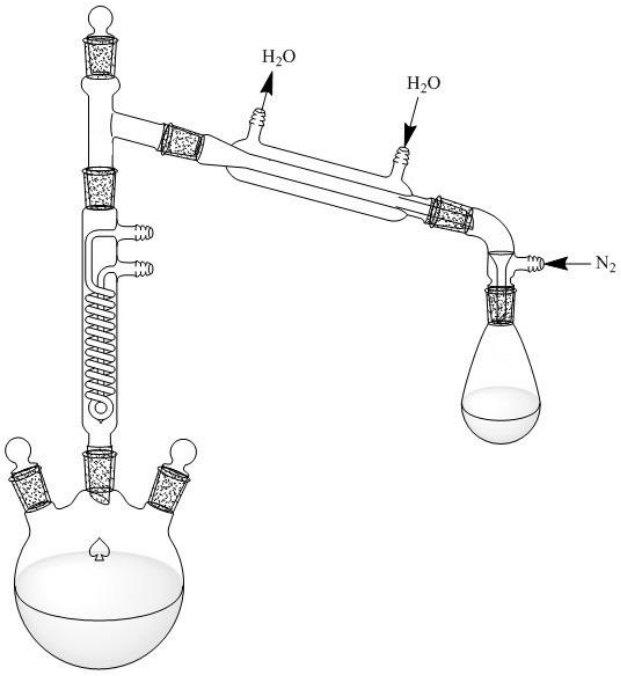

Figure 2.3.1 Experimental setup for melt polymerization of me-FDCA with EG

40 g of me-FDCA were charged together with 20 mL of EG into the three-neck round bottom glass reactor. Three cycles of vacuum/nitrogen were applied. The glass reactor was dipped into an oil bath and the heating plate was set at a temperature of 140 °C at a stirring speed of 600 rpm. In this way the mixture was slowly heated up until molten. Target temperature was reached in 25 minutes, at which time 0.50 g of catalyst (Bu_2SnO) were added to the mixture. EG (ca. 2.5 mL) was used to wash eventual catalyst stuck on the reactor wall. The system was heated to 180 °C and stirring speed was reduced to 380 rpm. Following 1 hour at 180°C pressure was reduced to 700 mbar. The pressure was reduced again after 40 minutes to 400 mbar and further to 200 mbar after 30 minutes. From this time on, system pressure was stepwise reduced until 10 mbar over a time of 40 min, with the mixture becoming very viscous. Temperature was increased to 200°C and the system was left under these conditions for 2 hours to ensure complete solidification of the mixture. The system was left under nitrogen atmosphere and once reached room temperature the solid product was removed ground with mortar and pestle to a fine powder, dried under vacuum at 50°C for 24h. The pre-polymer obtained was characterized with HPLC and GPC and subsequently used for other reactions without any additional purification.

2.3.2 Synthesis of cyclic-monomer by cyclo-depolymerization

A 250 mL three-neck round bottom glass reactor equipped with a magnetic stirrer, a thermocouple directly in contact with the reacting mixture and reflux condenser was connected to a Schlenk line with manifolds, directly connected to vacuum pump and nitrogen source.

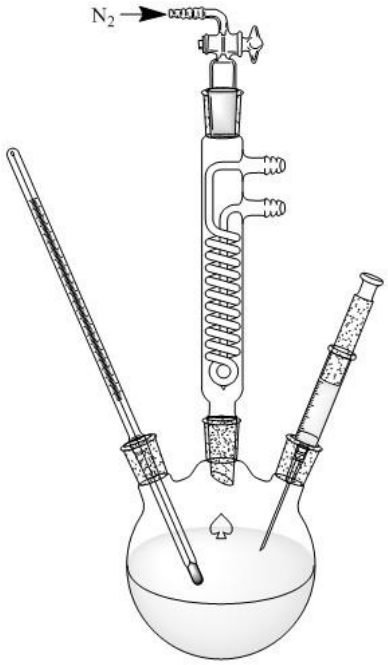

Figure 2.3.2 Experimental setup for cyclo-depolymerization

Pre-polymer (1 g) was charged into the flask and three cycles of vacuum/nitrogen where applied. During the vacuum step the glass reactor was heated using a heat gun. 100 mL of 2-methylnaphthalene was molten and subsequently added to the glass reactor. After solvent addition, the resulting solution was degassed with three cycles of vacuum/nitrogen and left under nitrogen atmosphere. The mixture was heated to 200 °C and the glass reactor was put into the oil bath. When the desired temperature was reached, a solution of 0.05 g dibutyltin oxide in mL tetraglyme was added to the system and the solution was left at that temperature for 3 hours. Samples were taken with a Pasteur pipette every 10 minutes for the first hour and every 30 minutes the remaining time. Each samples was analyzed by either HPLC, GPC or both.

2.4 Precipitation

2.4.1 Anti-solvent optimal ratio

Based on previous experiments, n-Hexane was used as anti-solvent for cyclo-depolymerization reactions. To estimate the optimal ratio anti-solvent/solvent eight different samples were prepared: each sample contained 1 mL of stock solution of DCM and dissolved reaction mixture. Different volumetric ratio anti-solvent/solvent were used: 5:1, 4:1, 3:1, 2:1, 1:1, 1:2, 1:4, 1:10. Each vial was prepared and let settle for 30 minutes, subsequently the contempt was taken with a syringe and filtered (mesh size: 0.45 µm). The two phases obtained were both transferred into crimp vials with different procedures: clear liquid phase was analyzed without dissolution in GPC solvent, while solid phase was dissolved and then analyzed.

2.4.2 Selective precipitation experiment

Following a typical cyclo-depolymerization experiment (section 2.3.2) the reaction mixture was cooled down from 200°C to a set temperature (50°C; 80°C; 90 °C or 100°C) and left for one hour at this temperature. Samples of the liquid phase were taken using a syringe with a 0.2 µm syringe filter during the cooling at intermediate temperatures, and after reaching the target temperature, every 10 minutes. Following the precipitation study, the reaction mixture was filtered at the set temperature and the solid phase analyzed by HPLC.

2.4.3 Complete precipitation experiment with n-hexane

All the experiments ended up with precipitation using hexane as an anti-solvent. The dilution ratio used was 3:1 (300 mL of hexane to 100mL of reacting mixture). After precipitation with n-hexane, mixture was filtered: solid phase was stored and together with the liquid phase analyzed.

2.5 Purification using Si-gel column chromatography

A flash chromatography column of 30 mm diameter was filled with DCM and slowly Si-gel was added to obtain a homogeneous slurry (~40 cm height). The mixture was left to settle for 1 hour and then residual solvent was removed keeping only a solvent layer of ca. 5 cm on top of the slurry phase. Solid product obtained from a depolymerization reaction was mixed with five spoons of Si-gel and slurried in DCM, some solvent was removed using a rotavapor. Subsequently, the slurry was placed on top on the Si-gel phase. Eluent was prepared using 900 mL of DCM and 100 mL of Et_2O. The raw product was eluted, fractionated and dried under vacuum.

2.6 Zeolite adsorption experiment

2.6.1 Batch adsorption of cyclic linear mixture on zeolites

A stock solution was prepared by dissolving 2 g of a cyclic linear polymer mixture obtained by depolymerization in 1L 10 vol% DEE in DCM. Four vials were filled with 5 mL each of the solution with the vials being weighted before and after addition to determine the liquid phase content. To each vial 25 mg of Zeolites CBV 780, HSZ-390HUA, HSZ-890HUA and HSZ-980HUA respectively were added and left for one hour to equilibrate. For each sample the liquid phase was measured and the solid content increased to 50 mg. Continuing this way the solid content was increased to 75, 100 and finally 150 mg.

2.6.2 Adsorption Experiment at reaction temperature

A typical depolymerization experiment was run as described in section 2.3.2. After 3 hours of reaction a defined amount of zeolites were added into the glass reactor using a funnel. Starting from the addition on, samples were taken with a syringe equipped with a filter (mesh size: 0.20 µm) every 10 minutes for the first hour and every 30 minutes until reaching the desired adsorption time.

2.7 Zeolite desorption experiment

2.7.1 Desorption experiment at room temperature

The solid phase used for adsorption experiments at room temperature (section 2.6.1) consisting of zeolites with species adsorbed on them was put in vials and filled with 30 mL of solvent made of 10% vol DEE in DCM. After 1 hour, the mixture was filtered and the liquid phase analyzed.

2.7.2 Desorption experiment at reaction temperature

Solid phase filtered from zeolite adsorption experiment composed of zeolites and adsorbed species was charged into a three-neck round bottom glass reactor with the same experimental setup of a cyclo-depolymerization reaction, together with 100 mL of solvent. Once charged solid phase and solvent three cycles of nitrogen/vacuum were applied to degas the liquid phase. Temperature was set at 200°C and kept there for 3 hours. Samples were taken with a syringe equipped with a filter (mesh size: 0.20 µm) and analyzed by HPLC. The investigated solvents were DCB, diphenyl ether, 2-MN and DMSO.

2.8 Zeolite column separation

Filtered solid phase obtained after adsorption experiment at reaction temperature (section 2.6.2) was charged in a flash chromatography column of 30 mm diameter. The column was filled with 1L of different solvents (10% vol of DEE in DCM, 10% vol of MeOH in DCM, pure MeOH). The liquid phase passed through the zeolite bed was analyzed by HPLC.

2.9 Adsorption/Desorption Experiments

A cyclodepolymerization reaction was run as described in section 2.3.2 and parallel five Schlenk tubes were heated to reaction temperature and charged with certain amount of zeolites under nitrogen atmosphere to avoid any water contamination. At the end of reaction, 2,5 mL of reacting solution was added in each tube and left until complete equilibration for one hour. After this time a filtered sample of the liquid phase was taken and analyzed and, to study desorption, 5 mL of fresh solvent were added. Following a filtered sample of the liquid phase was taken after one hour and analyzed.

2.10 Solubility studies

Eleven glass vials of 10 mL each were charged with a 50 mg of prepolymer together with 2 mL of solvent and heated up to different temperature into an heating block. After reached the target temperature the heating block was left there for 1 hour and, if dissolution was not occurring, two more mL of solvent were added. This procedure was repeated until complete dissolution for each temperature.

2.11 Cyclization via heterogeneous catalysis

2.11.1 Synthesis of cyclic-monomer using titanium-functionalized silica gel as heterogeneous catalyst

A 500 mL three-neck round bottom glass reactor was equipped with magnetic stirrer, a Dean Stark trap with a N_2 inlet, an additional-Liebig condenser on top and a small round bottom collection flask connected to the cooler through a drip tip of take-off second adapter. The two adapters were connected to the Schlenk line with manifolds to ensure a nitrogen atmosphere or to apply vacuum conditions.

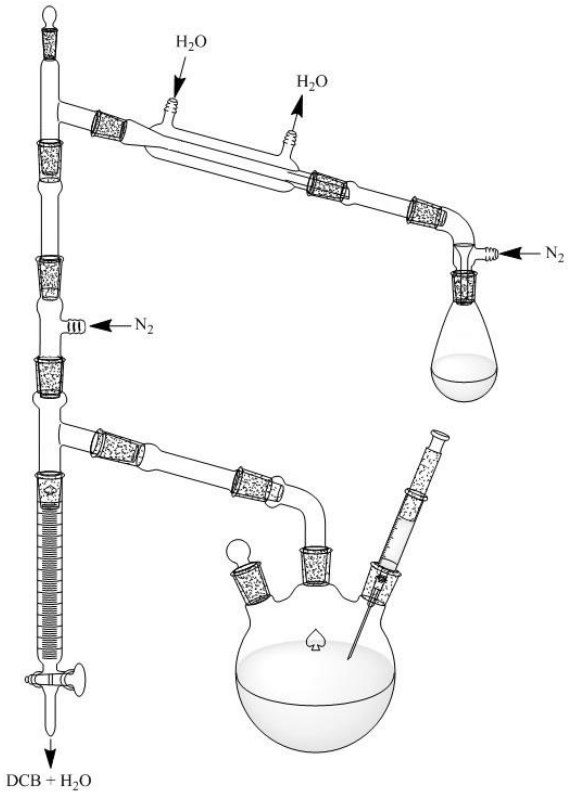

Figure 2.11.1 Experimental setup for functionalized Si-gel synthesis of cyclic-monomer

Three cycles of vacuum/nitrogen were applied prior to adding the reagents and then maintained under nitrogen flow.

150 mL of dichlorobenzene were charged together with 0.5 g of Si-gel, degassed with three cycles of nitrogen/vacuum, and subsequently heated up to reflux using an oil bath. In order to help condensation of DCB together with water adsorbed on Si-gel into the dropping funnel the junction lines were insulated with a double layer of glass wool and aluminum. Reaching the reflux temperature, 15 mL of DCB was distilled off from the dropping funnel. 0.5 mL of titanium isopropoxide was added after first distillation and then temperature was reduced to 110

°C for half an hour. A second fraction of 10 mL was taken from the Dean Stark trap before adding 1 g of pre-polymer. The last fraction of 20 mL was taken immediately after the pre-polymer addition. Reaction was run for three hours during which samples were taken each 30 minutes after pre-polymer addition and analyzed by HPLC.

3 Ring-Chain Equilibrium Model

Ring formation in polycondensation was already seen in the pioneering studies done by Carothers. Only in 1950, Jacobson and Stockmayer developed a model able to properly predict ring formation [1]. Their model was based on statistical thermodynamics in order to predict the equilibrium between linear polymer chains and their respective rings configuration. It is known that in a condensation polymer, a small percentage of product is organized in cyclic structures. By diluting such polymer it is possible to increase the probability of ring closure, and molecular weight. This theory was adopted for this project, with some changes, as a mathematical tool to estimate cyclic production.

3.1 Theory of Linear Systems. Jacobson & Stockmayer Equilibrium Model

In the work of Jacobson and Stockmayer, three different thermodynamically controlled stoichiometric types of polycondensation systems were considered in Figure 3.1.1.

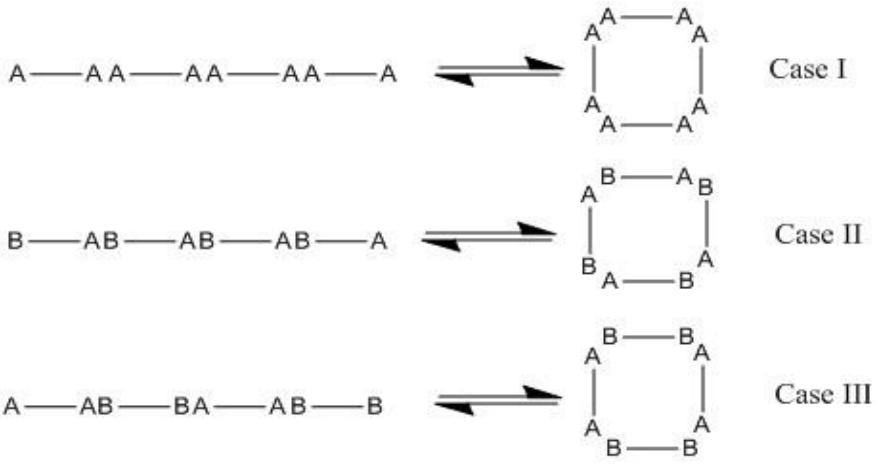

Figure 3.1.1 Representation of cases described in the model. Case I: identical monomer units, bearing two identical functional groups, A. Case II: identical monomer units, bearing two different functional groups, A and B. Case III: two different monomer units, each bearing two identical functional groups, A and B.

In this treatment the prepolymer used was considered to be a Case I polymer with EG being the side product released in the condensation reaction. In the theoretical treatment of Jacobson and Stockmayer the side product is omitted.

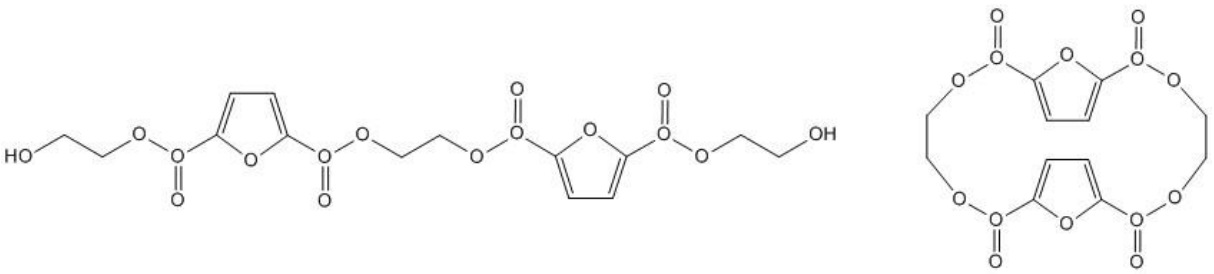

Figure 3.1.2 Linear and ring configurations of an oligomer of length two. In case of ring configuration, a molecule of EG is left apart to allow ring closure.

The model is based on two fundamental assumptions:

i. The reactivity of a functional group is independent on molecular size to which it is attached.
ii. The elementary steps in polycondensation are considered completely reversible.

Three additional assumption were made for model exploitation:

iii. Ring molecules must be long enough in order to neglect any steric effect. (> 15 skeletal atoms)
iv. Probability of ring closure can be expressed as a function of ring size, with the aid of the configuration theory for random coiled chains [56]
v. Chains and rings are in thermodynamic equilibrium

Flory [2] demonstrated hypothesis (i) to be valid for condensation systems. With this assumption, thermodynamic equivalence of all condensation bond in the system was postulated. Also assumption (ii) was experimentally demonstrated [58]. Attempts to derive a model on the basis of partial or total reversibility of elementary step reactions introduce non trivial mathematical complications without significant improvements. Assumption (iii) is fulfilled for cyclodepolymerization reaction: considering the smallest cyclic oligomer (C2), it is made by 26 skeletal atoms so it has a suitable length for this model. Nevertheless, the furanic repeating unit provide stiffness to molecular structure. Therefore the molecule might not assume a random coiled configuration. The validity of assumption (iv) will have to be checked experimentally. Thermodynamic equilibrium between chains and rings was experimentally proven in a previous study [34].

Once considered these assumptions to be valid, different quantities valid for the reacting system could be defined: the total number of monomer units: N, the total number of molecules (both cyclic and linear species): M, the total number of cyclic species: I and the total number of monomers in the cyclic fraction only: N'.

A molecular size distribution could be fully described on the basis of two parameters which are: C_n the n-mer cyclic species and L_n the n-mer linear species.

The previous quantities are related through the following mass balances:

$$\sum_{n=1}^{\infty}\left(C_n + L_n\right) = M \qquad \text{(Eq. 3.1)}$$

$$\sum_{n=1}^{\infty} n\left(C_n + L_n\right) = N \qquad \text{(Eq. 3.2)}$$

$$\sum_{n=1}^{\infty} n\left(C_n\right) = N' \qquad \text{(Eq. 3.2b)}$$

$$\sum_{n=1}^{\infty} \left(C_n\right) = I \qquad \text{(Eq. 3.3)}$$

3.1.1 Derivation of linear and cyclic polymer chain distribution

Once complete thermodynamic equilibrium is reached between cyclic and linear species, any subset of molecules such as the linear fraction will be in equilibrium within itself, thus a molecular size distribution of the same form as the distribution in the cyclic-free case [59] can be used for linear fraction:

$$L_n = Ax^n \qquad \text{(Eq. 3.4)}$$

Where A is the normalization constant and x is the fraction of reacted end groups in the linear fraction.

3.1.2 Derivation of Cyclic Fraction Distribution

Considering the general equation describing RCE:

$$L_{n+m} \rightleftharpoons C_n + L_m$$

The equilibrium constant of this global reaction in terms of number of molecules is:

$$K_{J\&S} = \frac{C_n L_m}{L_{m+n}} \qquad \text{(Eq. 3.5)}$$

The expression of linear fraction distribution can be introduced, leading to the following expression:

$$K_{J\&S} = \frac{C_n}{x^n} \qquad \text{(Eq. 3.6)}$$

In this way cyclic fraction distribution can be obtained.

The global change in Gibbs free energy, ΔG, is given by:

$$\Delta G = \Delta H - T\Delta S$$

Where ΔH and ΔS are reaction enthalpy and entropy respectively. The Gibbs free energy is related to equilibrium constant through the following equivalence:

$$-RTln\left(K_{J\&S}\right)=\Delta G \qquad \text{(Eq. 3.7)}$$

Since the reaction under analysis does neither involve a changes in the number of bonds nor in the type of bond, it can safely be assumed that it is attended by a negligible change of energy, so the only contribution to the equilibrium constant is the entropic one. This assumption of isenthalpic reaction and the entropic considerations will be deeper discussed in a following paragraph dedicated to thermodynamic aspects of the system. In order to obtain the final model those aspects are now left apart.

To better describe the entropy changes during the transesterification reaction, the reaction written above can be split into two elementary steps: the splitting of a chain of length $n + m$ into two chains of length n and m and the ring formation of a chain of length n.

$$L_{n+m} \rightleftharpoons L_n + L_m$$

$$L_n \rightleftharpoons C_n$$

Any byproducts are omitted because they do not appear in the overall reaction. The total entropic contribution can be evaluated as the sum of the entropy change of the two single reactions.

For the first reaction, the two atoms of the bond before breaking are confined into a small volume v_s, and after breaking, they could be distributed anywhere in the total volume V of the system. The symmetry number for a chain molecule is equal to 2, therefore, the entropy change is:

$$\Delta S_1 = k_b \ln\left(\frac{V}{2v_s}\right) \qquad \text{(Eq. 3.8)}$$

Where k_b is Boltzmann's constant.

The entropy change of the second reaction is given by the probability that the two chain end molecules are both located in the volume v_s, considering that symmetry number for n-mer ring is $2n$:

$$\Delta S_2 = k_b ln\left(\frac{P}{n}\right) \qquad \text{(Eq. 3.9)}$$

The probability *P* of ring closure for a randomly coiled chain was derived and will be briefly repeated here. Considering a chain with the length 1 the probability density distribution of possible end-to-end distances is given by the function:

$$W(l)\,dl = \left(\beta^3 \Big/ \pi^{3/2}\right)\exp\left(-\beta^2 l^2\right)4\pi l^2 dl \qquad \text{(Eq. 3.10)}$$

Where β is related to the mean square displacement length:

$$l^2 = \frac{3}{2\beta^2} \qquad \text{(Eq. 3.11)}$$

When a chain is closed to form a ring, the terminal chain atoms are constrained to volume v_s and the probability of this happening can be quantified by integrating *W(l)* over said volume:

$$P = \int_{v_s} W(l)\,dl \cong \left(\beta^3 \Big/ \pi^{3/2}\right)v_s \qquad \text{(Eq. 3.12)}$$

A convenient measure for the chain stiffness of a polymer, the so called effective link length b, can be defined and is given through

$$a = \frac{1+\cos(\alpha)}{1-\cos(\alpha)} n\nu b^2 \qquad \text{(Eq. 3.13)}$$

With *a* being the real link length and α real bond angle of the chain bonds. The effective length *b* is related to the mean square displacement length through the equation:

$$l^2 = \nu n b^2 \qquad \text{(Eq. 3.13a)}$$

Chain stiffness can be conveniently evaluated measuring the ratio between *b* to the actual link length.

Coupling Eq. 3.11 and Eq. 3.13a, a useful expression of β can be found:

$$\beta = \left(\frac{3}{2n\nu}\right)^{1/2}\left(\frac{1}{b}\right) \qquad \text{(Eq. 3.14)}$$

Substituting Eq.3.14 in Eq. 3.12, the fraction of chain configurations permitting ring closure is obtained:

$$P = \left(\frac{3}{2n\pi\nu} \right)^{3/2} \left(\frac{\nu_s}{b^3} \right) \qquad \text{(Eq.3.15)}$$

And with this the entropic contribution in Eq. 3.9 can be calculated. The summation of the two entropy contributions provides the total entropy change involved in the reaction, so the equilibrium constant is:

$$K_{J\&S} = \left(\frac{3}{2\nu\pi} \right)^{3/2} \frac{V}{2b^3} n^{-5/2} \qquad \text{(Eq. 3.16)}$$

The "bond volume" ν_s has been conveniently eliminated, making it unnecessary to quantify it.

Introducing Eq. 3.12 in Eq. 3.6 the result is the cyclic fraction distribution:

$$C_n = \left(\frac{3}{2\nu\pi} \right)^{3/2} \frac{V}{2b^3} n^{-5/2} x^n \qquad \text{(Eq. 3.17)}$$

Lumping some parameters into the term *B* an expression of cyclic fraction distribution shows the linear dependence of cyclic species with total volume of the system *V*, underling once more the importance of dilution for cyclization reactions.

$$B = \left(\frac{3}{2\nu\pi} \right)^{3/2} \frac{1}{2b^3} \qquad \text{(Eq. 3.18)}$$

$$C_n = BVn^{-5/2} x^n \qquad \text{(Eq. 3.19)}$$

3.2 Application of the model to a depolymerization systems

First, reaction involving linear chain species is taken into account. Considering a *n*-mer linear chain, it can react with a monomer specie to increase its length by one unit releasing EG as a byproduct.

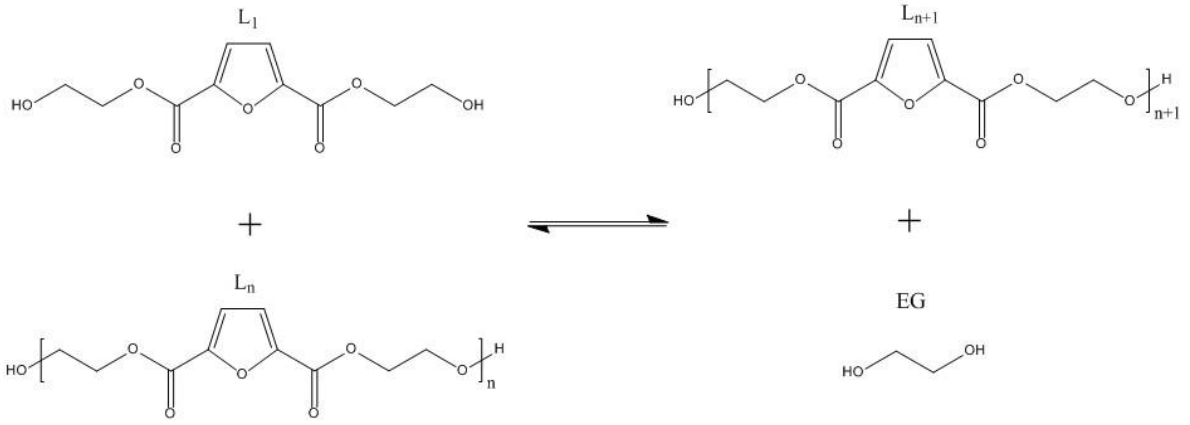

Figure 3.2.1General reaction of growing linear chains: a n-mer chain increases its length reacting with a monomer leading to a longer chain and producing EG as a side product

In general described as:

$$L_1 + L_n \rightleftharpoons L_{n+1} + EG$$

The equilibrium between the species involved is described by a constant K_L, which, under the assumption of independency from chain length, can be defined by the mass action law:

$$K_L = \frac{L_{n+1} EG}{L_1 L_n} \qquad \text{(Eq. 3.20)}$$

Writing the equation for chains with increasing repeating unit,

$$n = 1 \qquad L_2 = K_L \frac{L_1 L_1}{EG} \qquad \text{(Eq. 3.21a)}$$

$$n = 2 \qquad L_3 = K_L \frac{L_1 L_2}{EG} \qquad \text{(Eq. 3.21b)}$$

And substituting Eq. 3.21a into Eq. 3.21b one obtains:

$$L_3 = L_1\left(\frac{L_1 K_L}{EG}\right)^2 \qquad \text{(Eq. 3.22a)}$$

Grouping the quantities between brackets with a constant *a*:

$$L_3 = \frac{EG}{K_L}(a)^3 \qquad \text{(Eq. 3.22b)}$$

With: $$a = \left(\frac{L_1 K_L}{EG}\right) \qquad \text{(Eq. 3.23)}$$

Equation 3.22b can be generalized to:

$$L_n = \frac{EG}{K_L}(a)^n \qquad \text{(Eq. 3.24)}$$

Eq. 3.24 is mathematically similar to Eq. 3.4 with $A = \frac{EG}{K_L}$.

3.2.1 Cyclic Fraction Distribution

The second reaction taken into account is the one involving ring formation, from which the cyclic fraction distribution can be obtained. This kind of reaction is a reversible reaction in which a *n*-mer chain is in equilibrium with a *n*-mer ring giving as a byproduct a molecule of EG.

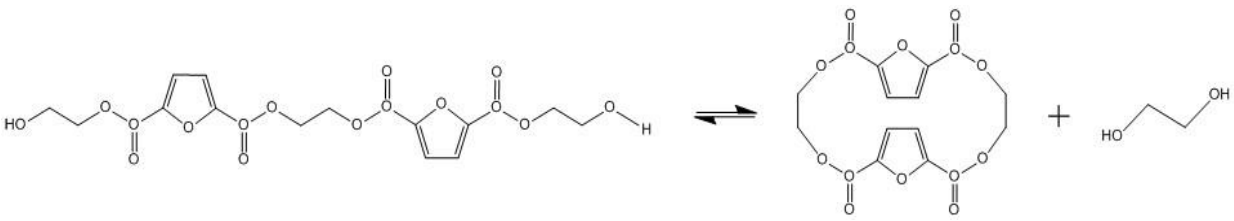

Figure 3.2.2 Ring formation reaction: a linear chain made by two FDCA molecules linked together closes up forming a cycle with the consequent release of a molecule of EG

Previous reaction involves a chain of two repeating unit, which is converted into a ring; in general this reaction can be written as:

$$L_n \rightleftharpoons C_n + EG$$

It can be demonstrated that this reaction is a linear combination of the reaction written in Jacobson and Stockmayer model:

$$L_{n+m} \rightleftharpoons C_n + L_m$$

And the reaction for chain growth equilibrium:

$$L_n + L_1 \rightleftharpoons L_{n+1} + EG$$

Two equilibrium constant are defined: one for the case under analysis K_C, and the previous one derived in the model Eq. 3.5. It is possible to relate them to obtain K_C as a function of $K_{J\&S}$.

$$K_C = \frac{C_n EG}{L_n} \qquad \text{(Eq. 3.25)}$$

$$K_C = K_L K_{J\&S} \qquad \text{(Eq. 3.26)}$$

Cyclic fraction distribution is rearranged from Eq. 3.25 that, matched with Eq. 3.26 and Eq. 3.24 lead to:

$$C_n = K_{J\&S} a^n \qquad \text{(Eq. 3.27)}$$

Which is similar, from a mathematical point of view, to Eq. 3.24: a standard Flory's distribution for polycondensing systems.

A global mass balance can be written considering the two building blocks involved: FDCA and EG.

$$EG_0 = \sum_{n=1}^{\infty} (n+1) L_N + \sum_{n=2}^{\infty} n C_n + EG \qquad \text{(Eq. 3.28)}$$

$$\phi_0 = \sum_{n=1}^{\infty} n L_N + \sum_{n=2}^{\infty} n C_n \qquad \text{(Eq. 3.29)}$$

The initial amount of ethylene glycol, EG_0, must be equal to the number of molecules of EG contained in linear fraction (first term), the ring fraction (second term) and the free EG.

Summation involving ring species starts from $n = 2$, since this is the smallest repeating unit of cycles.

As for EG, the initial furanic units: ϕ_0 are contained both in linear species (first term) and in cyclic species (second term).

Those two equations together with ring and linear fraction distributions provide a system of two equation in which the unknown parameters are: *a* and EG.

$$EG_0 = \frac{EG}{K_L}\sum_{n=1}^{\infty}(n+1)a^n + \sum_{n=2}^{\infty}BVa^n n^{-3/2} + EG \qquad \text{(Eq. 3.30)}$$

$$\phi_0 = \frac{EG}{K_L}\sum_{n=1}^{\infty}na^n + \sum_{n=2}^{\infty}BVa^n n^{-3/2} \qquad \text{(Eq. 3.31)}$$

An additional parameter K_1, was introduced to the system of equations to account for possible different reactivity of the monomer.

$$L_1 + L_1 \rightarrow L_2 + EG$$

To solve the final system of equations, K_L was assumed to be independent upon chain length apart from chains of length 1, this assumption has been shown to be valid also for other polycondensation systems such as PLA [60].

$$EG_0 = \frac{2}{K_L}EGa + \frac{K_1}{K_L^2}EG\sum_{n=2}^{\infty}(n+1)a^n + \sum_{n=2}^{\infty}BVa^n n^{-3/2} + EG \qquad \text{(Eq. 3.32)}$$

$$\phi_0 = \frac{1}{K_L}EGa + \frac{K_1}{K_L^2}EG\sum_{n=1}^{\infty}na^n + \sum_{n=2}^{\infty}BVa^n n^{-3/2} \qquad \text{(Eq. 3.33)}$$

The two equations can be easily solved for EG and rearranges a one function of *a*:

$$EG = \frac{EG_0 - \sum_{n=2}^{\infty}BVa^n n^{-3/2}}{\left(\frac{2}{K_L}a + \frac{K_1}{K_L^2}\sum_{n=2}^{\infty}(n+1)a^n + 1\right)} = \frac{\phi_0 - \sum_{n=2}^{\infty}BVa^n n^{-3/2}}{\left(\frac{1}{K_L}a + \frac{K_1}{K_L^2}\sum_{n=2}^{\infty}(n+1)a^n\right)} \qquad \text{(Eq. 3.34)}$$

This function can be solved numerically for *a,* from which in return all quantities in the system can be calculated.

The independent variables in this system are *a* and *EG*. The experimental input parameters are reaction volume *V* and the ratio of *EG* over *FDCA*.

3.3 J&S model applied to selective adsorption experiments

It is possible to include adsorption directly into the model previously described allowing the estimation of the final purity obtained.

Mass balances need to be modified in order to take into account species adsorbed on the adsorbent medium. For this system, a step isotherm is considered since adsorption is very strong and fast.

The adsorption mechanism can be described by two reactions:

$$L_n \rightleftharpoons L_n^*$$

$$EG \rightleftharpoons EG^*$$

In which both linear species and ethylene glycol are adsorbed. An equilibrium constant k^* can be introduced and maintained fixed for both reactions.

The two previous equations (Eq. 3.28 and Eq. 3.29) can still be valid introducing in the balance also the species captured in the adsorbent:

$$EG_0 = \sum_{n=1}^{\infty}(n+1)L_n + \sum_{n=2}^{\infty} nC_n + EG + EG^* + \sum_{n=1}^{\infty}(n+1)L_n^* \qquad \text{(Eq. 3.36)}$$

$$\phi_0 = \sum_{n=1}^{\infty} nL_n + \sum_{n=2}^{\infty} nC_n + \sum_{n=1}^{\infty} nL_n^* \qquad \text{(Eq. 3.37)}$$

It is possible to know the amount of adsorbed species by writing a mass balance directly on the adsorbent medium:

$$K_{ADS}^* m_{zeol} = \sum_{n=1}^{\infty} M_{Ln} L_n^* + M_{EG} EG^* \qquad \text{(Eq. 3.38)}$$

In which: m_{zeol} is the mass of zeolites, M_{Ln} and M_{EG} are the molecular weight of the adsorbed species and K_{ADS}^* is the loading capacity defined by grams of adsorbed species per gram of adsorbent. Since all the balances are written per unit of molecules, K_{ADS}^* has to be multiplied by the Avogadro's number $\left[\frac{molecule}{mol}\right]$ in order to fulfill the dimensional analysis:

$$\left[\frac{g_{ADS}}{g_{zeol}}\right]\left[g_{zeol}\right]=\left[\frac{g_{Ln}}{mol_{Ln}}\right]\left[molecule_{Ln}\right]\left[\frac{mol}{molecule}\right]+\left[\frac{g_{EG}}{mol_{EG}}\right]\left[molecule_{EG}\right]\left[\frac{mol}{molecule}\right]$$

It is interesting to note that solving the system of equations (Eq. 3.36 Eq. 3.37 and Eq. 3.38) for the parameter *a*, the mathematical expression is independent upon adsorption. This clearly means that adsorption is not affecting chain length, more over is not involved in reaction.

Solving the system mentioned above it is possible to estimate the equilibrium constant of adsorption k^*, with which is possible to evaluate the mass of adsorbed species.

The loading capacity can be experimentally obtained and subsequently exploited to solve the system of equations; it is also possible to directly use the mathematical expression of the isotherm governing the adsorption phenomena to better predict the final equilibrium.

3.4 Thermodynamics aspects

Following from the assumption that reactions take place without changing bond number, Gibbs free energy was evaluated only by entropic contributions.

As many authors did [47], it is however reasonable to consider rings strain and heat of cyclization to better estimate Gibbs free energy of reaction: this way both entropy and enthalpy of cyclization contribute.

3.4.1 Entropic contributions in J&S theory

Entropic contributions are evaluated on the basis of statistical thermodynamics, evaluating the probability of a reaction to take place.

Considering the whole reacting volume V, one single chain can undergo a cyclic formation reaction: the global reaction can be split into two elementary steps as it was done for developing Jacobson and Stockmayer model.

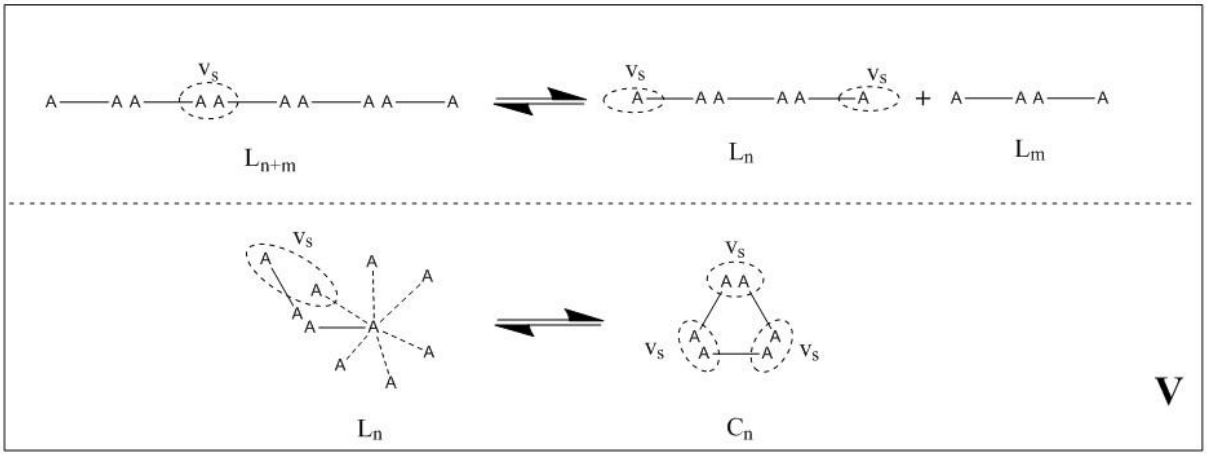

Figure 3.4.1 Molecular scheme reaction. First step involves chain breaking into two smaller parts, the second one in which the molecule has to rearrange on itself to form a cycle.

In order to have reaction two end groups must be in the same volume v_s swept out by a bond, thus can be associated a probability that a linear *n*-mer has a configuration suitable for cyclization: the ratio of the number of configurations of the ring to that of the corresponding linear molecule.

Reaction I: $L_{n+m} \rightleftharpoons L_n + L_m$

For a chain of length $n+m$ probability is equal to one since the two atoms are linked together into a bond.

When this chain breaks up, it is split into two smaller chain moving in the reacting volume freely: probability of end groups to be in the same volume v_s is $\frac{2v_s}{V}$ since both end groups are available for reaction.

Thus, entropy change associated to bond breaking is:

$$\Delta S_1 = k_b \ln\left(\frac{V}{2v_s}\right)$$

Reaction II: $L_n \rightleftharpoons C_n$

Considering the ring, probability is again one because atoms are bounded in the same volume v_s multiplied *n*-times, one per each bounded end groups. The chain molecule has to rotate on itself in order to close up, this is exactly the probability written in Eq. 3.12. The ratio of the number of configurations for C_n relative to L_n is simply the probability of L_n closing on itself.

Entropy change can be evaluated as:

$$\Delta S_2 = k_b \ln\left(\frac{P}{n}\right)$$

To sum up, in Jacobson and Stockmayer theory there are two contributions to entropy change:

- A positive one due to the dissociation of one molecule into two increasing the center of mass freedom. Before the bond breaks, the two segments are restricted to lie within a small distance from one other, but after the bond breaks, they may be at any distance from one another, limited only by sample volume, *V*.
- A negative one due to the decreased number of configurations on going from a linear chain to a linear and a cyclic product. The number of configuration available for cyclic C_n is a small subset of those available for the linear *n*-mer chain.

The reduction in configurational entropy increases for ring size *n* but is independent of residual chain length *m*.

4 Results and Discussions

The chapter is divided in two main parts: synthesis of cyclic oligomers and their subsequent purification.

In the first one the cyclodepolymerization reaction is further investigated. The application of calibration curves gives the possibility to obtain a quantitative analysis of the final product and generates reliable experimental data to validate the mathematical model able to describe the reaction equilibrium. Moreover, different solvents are screened in order to switch from the previous solvent to an easier to handle one, with the aim of obtaining a more sustainable process.

In the second part, the purification of the produced cyclic oligomers is investigated, showing the possibility of using zeolites as selective adsorbent to obtain a final product suitable for ring opening polymerization.

4.1 Analytical Aspects

Depolymerization reactions result in a distribution of both linear and cyclic oligomers. In a previous work, SEC was used to characterize the products. The purity of cyclic species was defined via the peak area percentage. This approach proved to lead to some inconsistences in the results. More specifically, even if the SEC resolution was good enough to see individual linear species, there was some overlap for the linear and the cyclic oligomer with repeating unit two, as shown in Figure 4.1.1. This lead to an overestimation of the depolymerization yield.

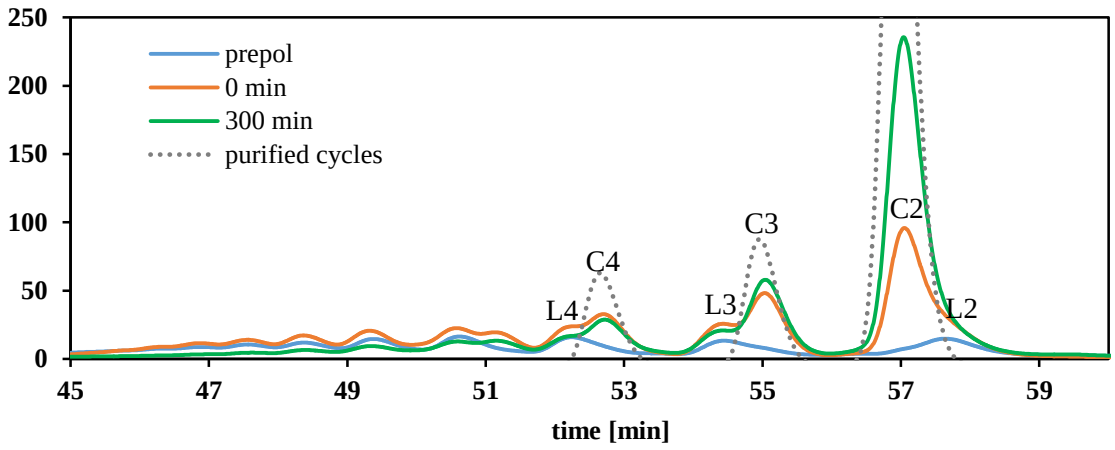

Figure 4.1.1 SEC plot showing four different traces: the initial prepolymer, purified cycles and reaction at the time corresponding to catalyst addition (0min) and the one corresponding to the end of reaction (300 min). The overlapping of the peaks corresponding to linear and cycles of repeating unit 2 is clearly visible.

In order to characterize both qualitatively and quantitatively each component, High Performance Liquid Chromatography (HPLC) was used to analyze the reaction products. In a previous work, the characterization of every peak was performed by HPLC-MS to determine the mass of each species and NMR to determine the chemical composition. Using this approach, a complete characterization of the composition in a depolymerization mixture was available.

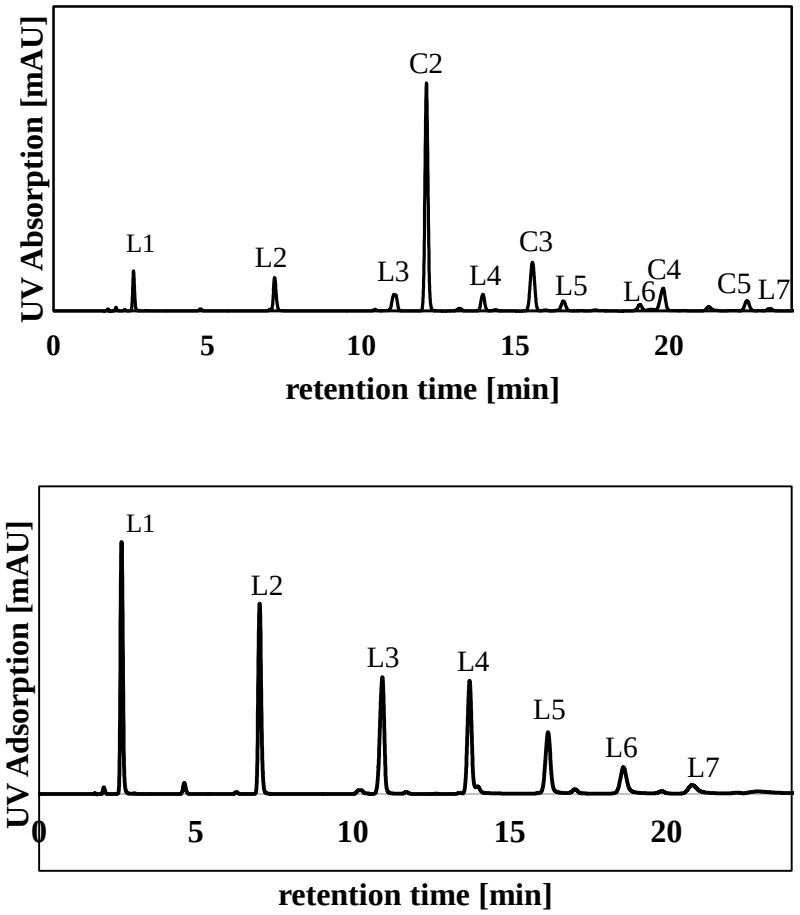

Figure 4.1.1 Top figure shows a typical plot of a cyclodepolymerization reaction: linear and cycles are labelled with L and C followed by the number of repeating units. The bottom plot shows the distribution of linear species in the prepolymer.

Finally, a calibration provided quantitative data of composition. The calibration curves for a distribution of cyclic oligomers and the pure cyclic dimer are shown in Figure 4.1.2. Since both calibration curves overlap and show a linear behavior, it can be safely assumed that the calibration factor is the same for all cyclic species. Good linearity and similar calibration constant were also observed for a distribution of linear oligomers.

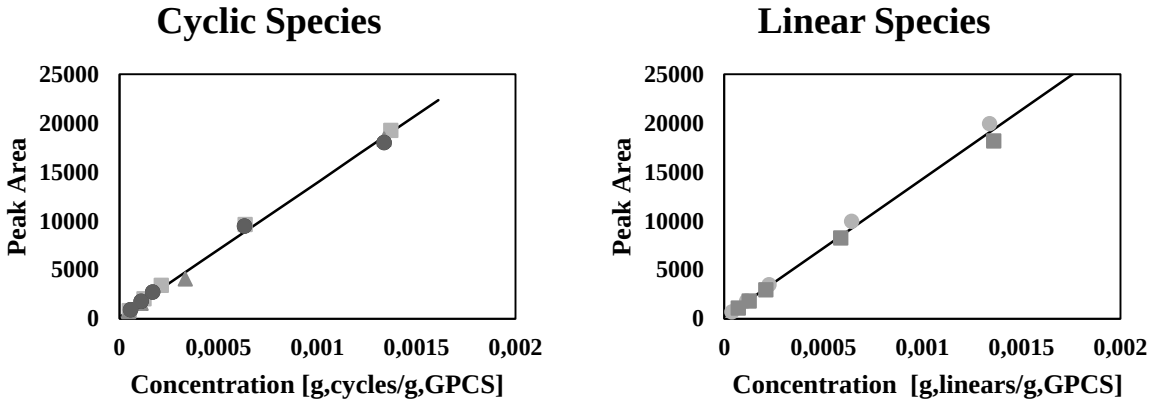

Figure 4.1.2 Experimental data and calibration curves of the two species involved: cyclic and linear.

The picture was different for the solvents used for the depolymerization reactions. The calibration curves for 2-methylnaphthalene showed peak saturation at higher concentrations while the other solvents were generally linear. With reference to the solvent 2-MN, the following equation applies:

$$\frac{1}{C_{2MN}} = a\frac{1}{Area^{2.79}} + b\ ;$$

where C_{2MN} is the concentration of 2-MN and *Area* is the area of the solvent peak. The calibration curve for dichlorobenzene and diphenyl ether are shown in Figure 4.1.3. Using the solvent as an internal standard for the analysis of the reaction mixtures, the total amount of dissolved species could be reliably evaluated.

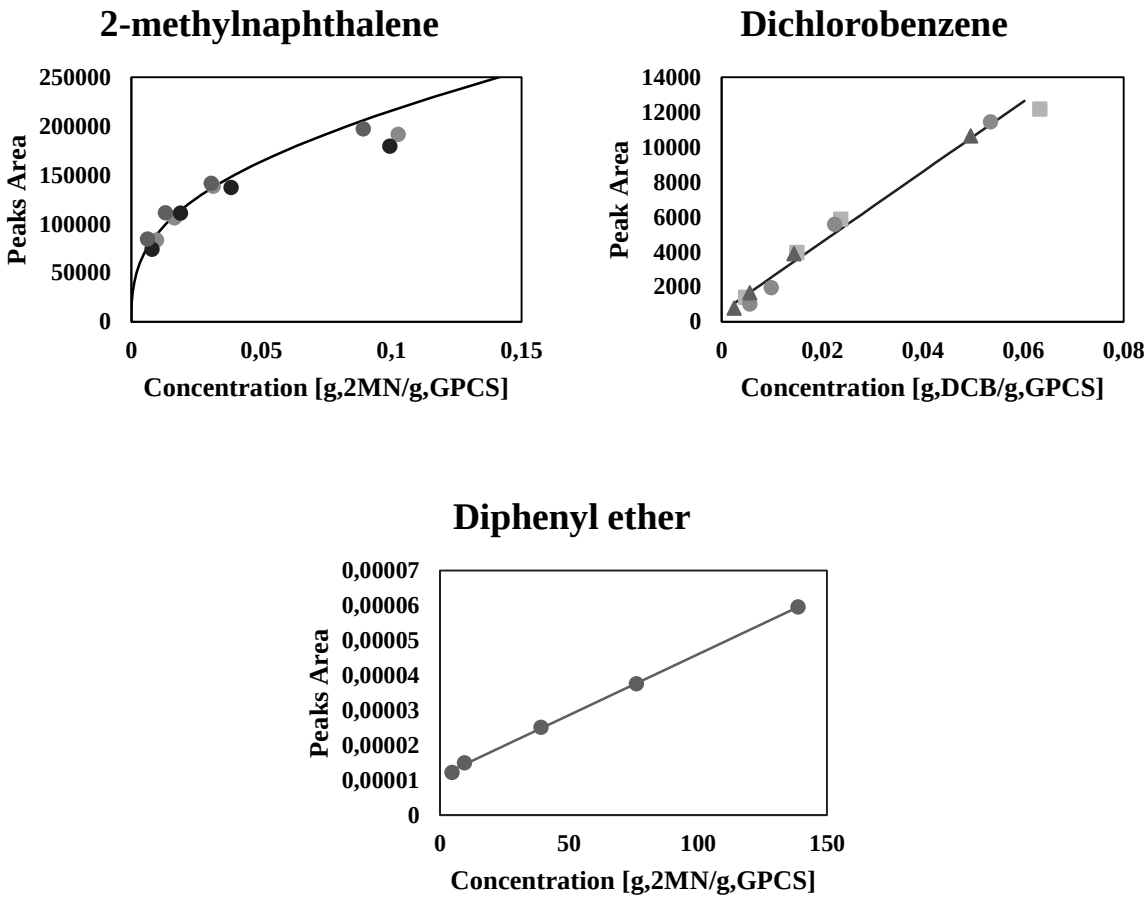

Figure 4.1.3 Experimental data and calibration curves for the solvents employed in different reactions.

The estimated values of the calibration parameters corresponding to the curves in the figure above are summarized in Table 4.1.1.

Table 4.1.1 Calibration parameters for different solvents

	a	**b**
2-methylnaphthalene	-5.05586E+15	-1.31
Diphenyl ether	3.48943E-07	1.119E-05
Dichlorobenzene	200796	554.1133

The range of tolerance employed for all the calibration curves is 10 %.

4.2 Synthetic Considerations

The raw material needed for the cyclodepolymerization reactions was synthesized according to the experimental procedure described in section 2.2.1. Through this step, short oligomers of polyethylene furanoate were formed while methanol was removed. To increase the conversion, the process is run under vacuum (10 mbar). It was seen that the application of vacuum should not be done in the early stage of the reaction, when most of the EG is unconverted and would be easily removed by vacuum. Nevertheless, leaving the reaction at atmospheric pressure for too long leads to a slight coloring of the prepolymer, which is a sign of slow degradation at the reaction temperature. Three different prepolymers were produced during this work, which show slight differences in composition.

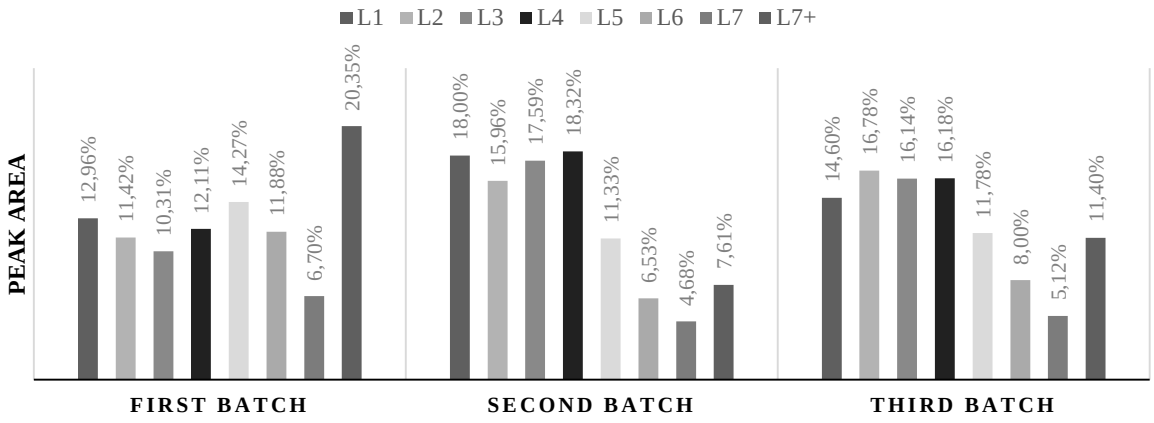

Figure 4.2.1 Compositions of three different prepolymers. L1 to L7+ are prepolymers composed of n-repeating units of EG-FDCA-EG from 1 to the sum of chains containing more than 7 repeating units

	First Batch	Second Batch	Third Batch
Final prepolymer mass [g]	44.28	44.19	49.65

The first batch had a higher percentage of longer chains, while the second and third one have a shorter average length. Long chains are shortened by EG removal under vacuum that was much more effective on the second and the third batches. Third batch was discarded because pressure reduction was not fast enough and the pressure required was not reached, ending up with a product that at first look was not suitable for depolymerization reaction; moreover, during

reaction the mixture did not become solid, meaning that EG removal was not effective. All reactions were carried out using first and second batches; the difference in composition was taken into account when the model was applied to predict the final equilibrium.

4.3 Cyclodepolymerization Reactions

The reaction protocol for synthesizing cyOEF by depolymerization was already established in a previous Master Thesis. The same approach was applied also in this work with the exception that analyses were carried out by HPLC. A reaction was carried out in 2-methylnaphthalene at 200ºC with prepolymer concentration of 10g/L. HPLC was a reliable tool to monitor the reaction evolution in time: in fact, each single species could be detected with good resolution. In Figure 4.3.1, HPLC traces at 4 different times are shown:

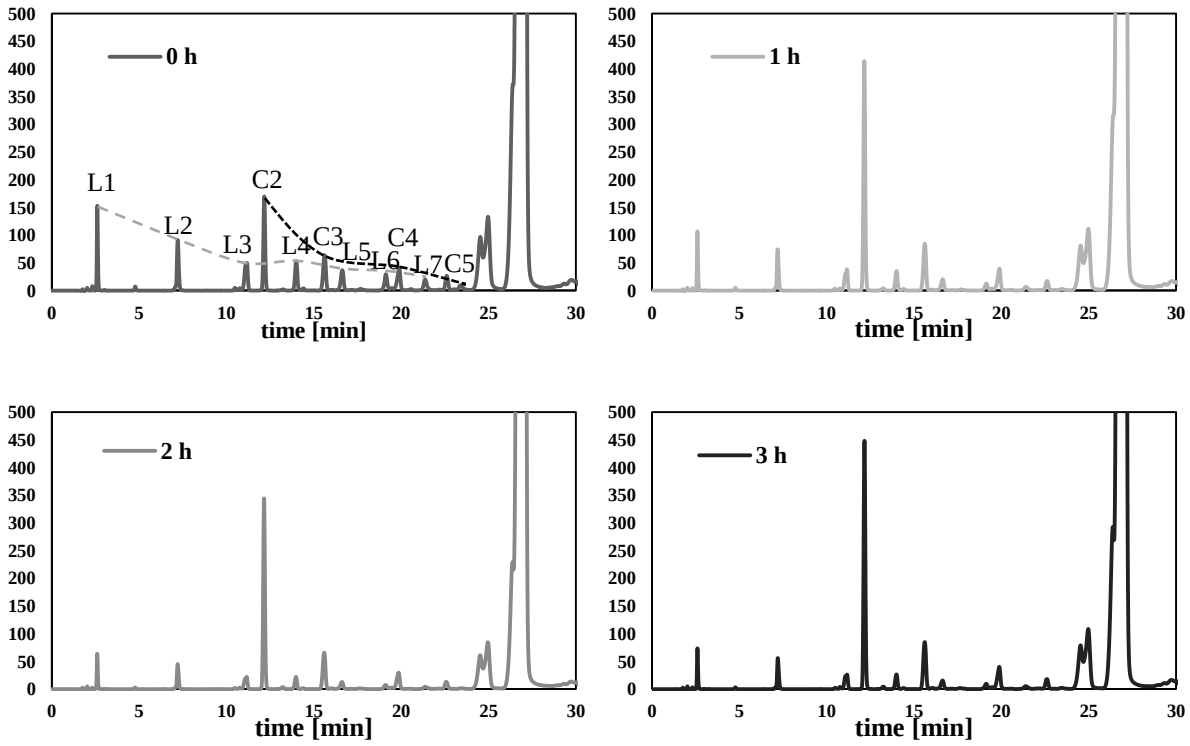

Figure 4.3.1 HPLC traces at four different times: time 0h corresponds to the achievement of reaction temperature of 200°C.

Qualitatively, the peaks corresponding to the linear chains decrease relative to those of the cycles. To quantify the extent of such reduction (i.e. how much linears are converted into cyclic

oligomers), the calibration curves developed above were used, thus obtaining the results shown in Figure 4.3.2. It can also be observed, that the mass of prepolymer charged into the reactor (1 g) is well predicted by the calibration used. The total mass of reaction predicted is around 1000 mg, as shown in the first plot (Figure 4.3.2).

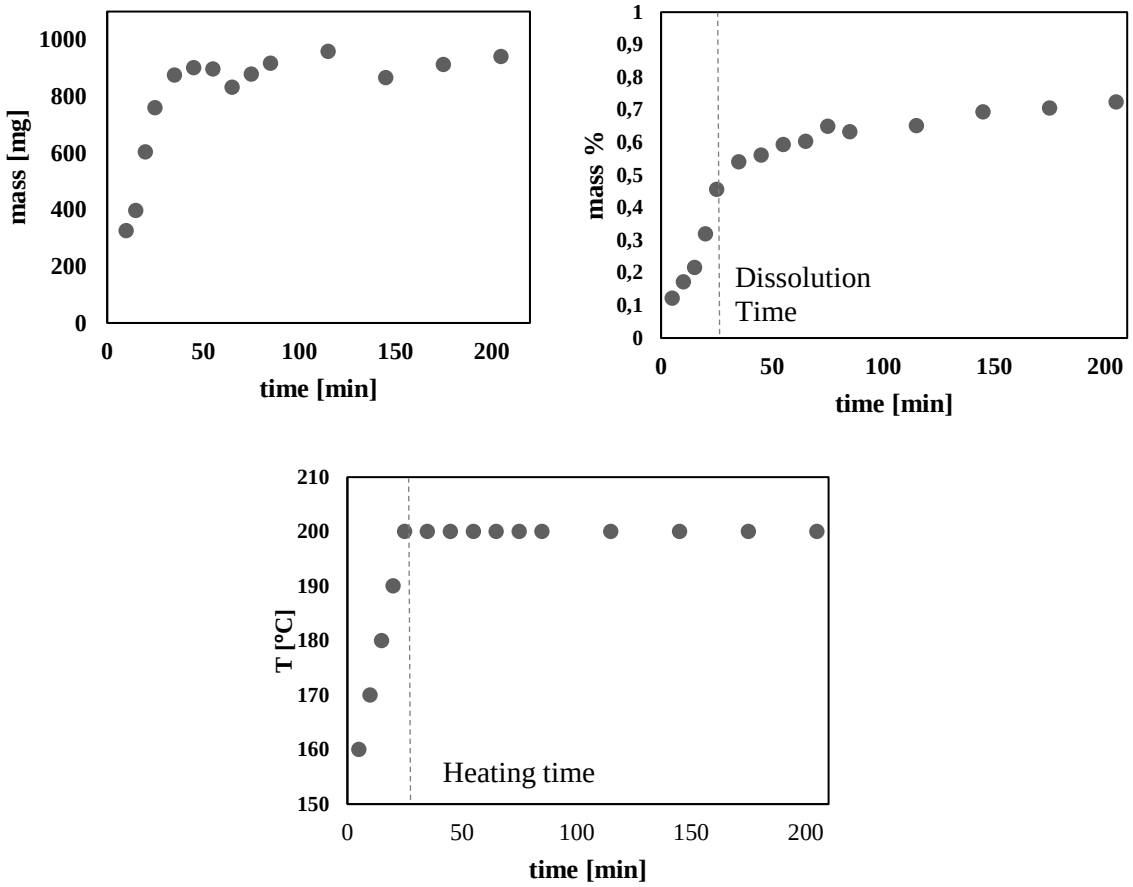

Figure 4.3.2 Top: total mass in the liquid phase vs. time and mass percentage of cyclic species with respect to (linear+cycles) vs. time. Bottom: temperature profile vs. time.

In Figure 4.3.2, the cyclic mass fraction as a function of time was evaluated as the mass of cycles with respect to the sum of both linear and cyclic species:

$$m_{cycle}\% = \frac{m_{cycle}}{m_{cycle} + m_{linears}}$$

The initial pre-PEF contained a negligible amount of cyclic species. As soon as such prepolymer starts to dissolve, the chains are converted into cycles. Notably, most of the reaction takes place during the dissolution of the prepolymer: once reached reaction temperature, where the dissolution of the prepolymer is complete, the reaction mixture approaches an equilibrium

between cyclics and linears. Such equilibration is quite slow and the percentage increase of cyclic products is only about 20%.

The reliability of the calibration was assessed by comparing the results with those obtained through a *direct calibration*: each sample was weighed to know exactly the amount of reacting mixture contained and compared with the mass predicted by calibration using the peak area of the solvent as an internal standard. The results collected following the two approaches are shown in Figure 4.3.3, and they are nicely superimposed. Therefore, all the results reported in the following have been obtained by the internal standard calibration.

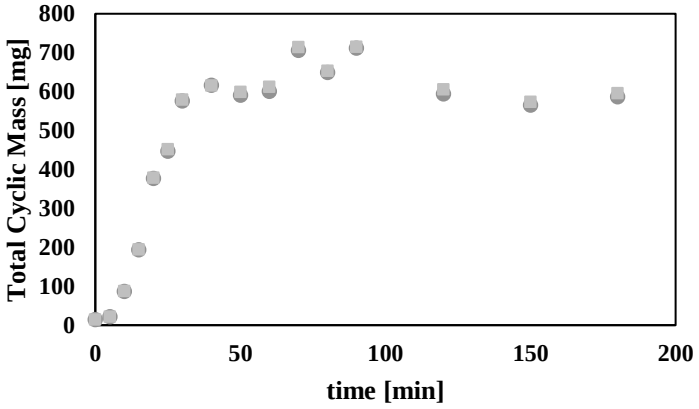

Figure 4.3.3 Total mass of cyclic species during reaction. Comparison between the data evaluated by direct calibration (●) and internal standard calibration (■)

4.3.1 Catalyst Influence

The role of the catalyst was preliminarily studied in a previous Master Thesis, showing a general promising trend in the case of tin-based catalysts [61]. The two catalysts which performed best in terms of conversion are stannoxane and dibutyltin oxide.

Comparing two different reactions carried out at standard conditions (prepolymer concentration of 10 g/L, solvent 2-MN, reaction temperature 200ºC) with (5%wt of dibutyltin oxide) and without catalyst, the negligible influence of the catalyst on the rate of approach to the reaction equilibrium was made clear.

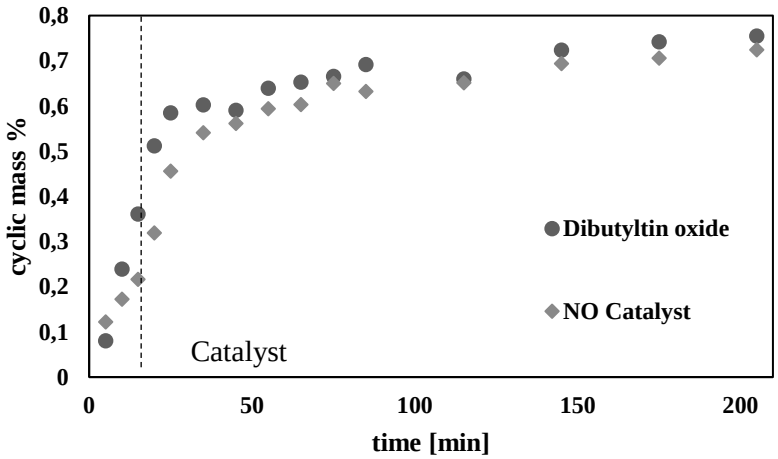

Figure 4.3.4 Time evolution of the cyclic mass fraction with and without catalyst

The equilibration without catalyst proceeded until the final conversion of about 70%. In the case of cyclization without catalyst, one has to consider that some residual catalyst remaining into the solid prepolymer could also affect the reaction rate. In any case, given these results, all the reactions carried out in the following were run without catalyst.

4.4 Solvent Screening

4.4.1 Solubility study

The solvent applied throughout most of this work, 2-MN, was selected because of the good solubility of reactants and products at the high temperatures required for the synthesis. Moreover, good conversion was measured in the depolymerization reaction run in this solvent in previous experiments. Furthermore, in a recent 10 L scale up of the reaction carried out by the industrial partner of this project, said solvent was applied. Therefore, this was also the solvent studied most during this work. Nevertheless, this solvent is also exhibiting serious drawbacks such as high melting temperature forcing to perform hot filtration and high boiling temperature that impeded solvent evaporation from filtered products. The only possibility of removing this solvent from the final product was by washing it with an auxiliary solvent. All these reasons make it not convenient to its use at the industrial scale. Therefore, a brief solubility screening was run on alternative, industrially applicable solvents in view of their use in depolymerization. The results of this solubility study are summarized in Table 4.4.1.

Table 4.4.1 Summary of the solubility study: the amounts of dissolved prepolymer at the corresponding temperature are reported. "No dissolution" means that the amount of prepolymer dissolved was not enough to be detected. Solubility studies were performed at atmospheric pressure thus never above the boiling temperature of the solvent (>T_B)

		T_B	110°C	140°C	170°C	200°C
Aromatic Solvents	Diphenyl Ether	258°C	No dissolution		~8.3 g/L	>400 g/L
	2-MN	241°C	No dissolution		~8 g/L	~400 g/L
	Nitrobenzene	210°C	No dissolution		~8.3 g/L	> 400 g/L
	DCB	180°C	No dissolution		~5 g/L	> T_B
	p-xylene	138°C	~4 g/L	> T_B	> T_B	> T_B
Polar Aprotic	DMSO	189°C	~200 g/L	<400 g/L	1250 g/L	> T_B
	DMF	153°C	211 g/L	350 g/L	> T_B	> T_B
Ionic Liquids	Pyr13TFSI [IL]	300°C	No dissolution		~8 g/L	> 465 g/L

The solvents studied in this screening could be divided into three groups: aromatic solvents, polar aprotic solvents and ionic liquids. The current solvent employed for cyclodepolymerization belongs to the group of aromatic solvents, in which solubility is low until the pre-polymer melting temperature (~210ºC [33]) is approached. At this point very high amount could be dissolved. The only solvent in which prepolymer was partially solubilized at low temperature was p-xylene but only at low concentration (around 4 g/L). It is interesting to notice that solvents containing Nitrogen showed a yellowish color at high concentrations, while the other solvents remained colorless.

Polar aprotic solvents were solubilizing pre-polymer even at low temperatures. Between the two investigated solvents, DMSO was exhibiting an extremely high solubility even at 170°C. DMF was also exhibiting good solubility but could not be used at 170°C due to its low boiling point. The solution remained colorless and transparent even at very high concentrations.

The last solvent investigated was selected among the ionic liquids due to their chemical stability at high temperatures and the growing interest in their use as chemical solvents. Dissolution was only seen at temperatures approaching the melting temperature of the prepolymer, where large amounts could be dissolved. In general, their behavior was similar to that of aromatic solvents.

4.4.2 Cyclodepolymerization reactions in different solvents

Once studied the solubility of the pre-PEF, four solvents were further investigated to be used for cyclodepolymerization. Their specific properties in terms of sustainability, processing and solubility made them suitable solvents for this specific process step. The selected four solvents are: diphenyl ether, dichlorobenzene, dimethyl sulfoxide and tetraethylene glycol dimethyl ether. A summary of the experimental conditions of the reactions carried out in the different solvents is provided in Table 4.4.2.

Table 4.4.2 Summary of reaction conditions of cyclodepolymerization reactions run in different solvents

Solvent	Reaction T [ºC]	Pre-PEF concentration [g/L]	Catalyst
Dichlorobenzene	170-190-200	5	No
Diphenyl ether	200	10 and 5	No
DMSO	130-170	10	No/Bu_2SnO
t-glyme	200	10	No

Let us list a few comments about the depolymerization behavior case by case.

Tetraethylene glycol dimethyl ether

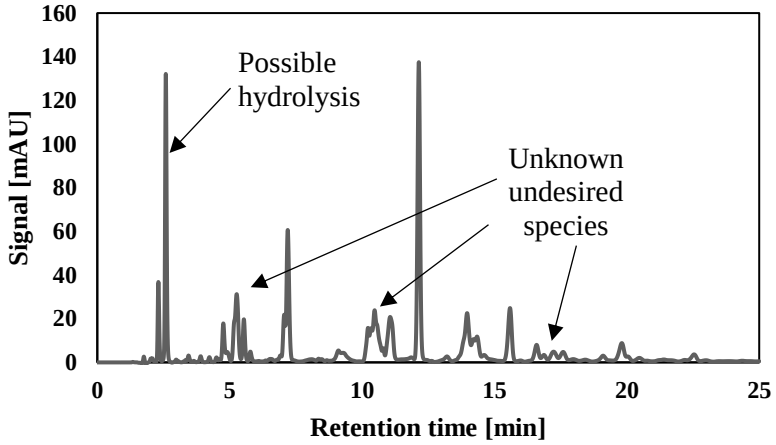

Figure 4.4.1 HPLC trace of cyclodepolymerization after 3h reaction time using t-glyme as solvent showing the presence of undesired species and possible hydrolysis side reaction.

The first solvent investigated was t-glyme, chosen because of (i) its large solvent power at high temperature and (ii) its previous use as effective plasticizer in the ring opening polymerization step, thus aiming to apply the same solvent for both steps, depolymerization and ring-opening. Note that the use of the same solvent for both monomer synthesis and subsequent polymerization could facilitate the purification procedure: if the final product contains some solvent left, it can be exploited instead of removed. A strict removal of the solvent is not compulsory.

Pre-PEF immediately dissolved as the temperature was approaching 200°C; the solution remained transparent and colorless until the end of the reaction. However, as shown in the HPLC trace in Figure 4.4.1, t-glyme demonstrated its unsuitability for the reaction: during the synthesis the solvent showed instability favoring formation of unknown species and decomposition of the PEF chains. Moreover, the presence of small traces of water in the solvent greatly promoted hydrolysis reaction, thus degrading the initial reactant. For these reasons, t-glyme was discarded without any further study.

Dichlorobenzene

DCB was already used for reactive distillation to synthetize cyOEF, proving its feasibility in cyclic synthesis. The main advantage of dichlorobenzene with respect to 2-methylnaphthalene is its lower boiling point (179°C instead of 240°C), enabling an easier solvent removal from the final product by devolatilization.

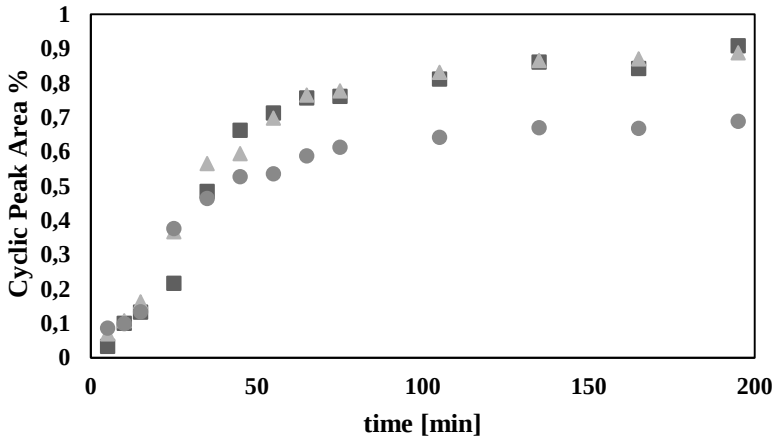

Figure 4.4.2 Evolution of the percentage peak area of cyclic species in cyclodepolymerization reactions using dichlorobenzene as solvent and considering different temperature: (●) 170°C, (■) Reflux temperature (179°C), and (▲) 190°C.

During the depolymerization reaction at 170°C, the prepolymer dissolution was poor. Nevertheless, the percentage of cyclic species with respect to the sum of linear and cyclics in the liquid phase reached values around 70%. Increasing the temperature to reflux conditions, enhanced dissolution of pre-PEF and larger percentage values were achieved, about 90%. On the other hand, going further above the boiling temperature of DCB, such percentage remained almost constant. Even if the solubility was quite poor, dichlorobenzene appears to be a promising solvent able to promote cyclics synthesis from a prepolymer mixture.

Diphenyl ether

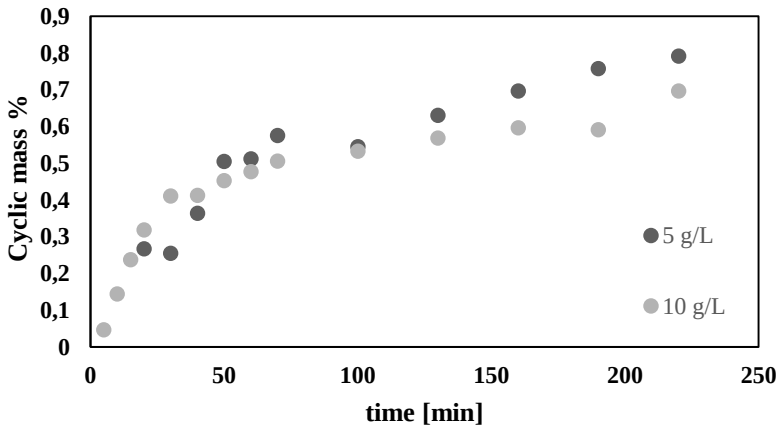

Figure 4.4.3 Dilution effect in cyclodepolymerization reactions in diphenyl ether. Equilibrium cyclic mass percentage increases when dilution decreases.

Prepolymer solubility in Phenyl-Ether was high, especially at temperature close to 200°C. Diphenyl ether showed some important advantages: the solution remained clear and transparent during the reaction, while with 2-methylnaphthalene the color was turning yellowish leading to a final colored product. Additionally, the melting temperature of diphenyl ether is 26°C while 2-MN is 42°C: accordingly, the solvent would be liquid rather than solid in the following purification steps slightly above room temperature, thus simplifing the procedure.

By comparing the mass percentage of cyclic species at equilibrium in Phenyl-Ether and in 2-MN, the final range of yield values is quite similar and close to 70%. Furthermore, the dilution effect is demonstrated also in this case: reducing the concentration of initial pre-polymer, the final yield is higher. For all the reasons above, this solvent has been identified as a viable alternative to 2-MN.

Table 4.4.3 Final equilibrium composition of three different reaction with diphenyl ether as solvent and reaction temperature of 200ºC.

Depolymerization Conditions	Cyclic purity %
5 g/L (3h)	79.16
10 g/L (3h)	69.61

Dimethyl sulfoxide

The high solubility of the raw pre-polymer in DMSO disclosed the possibility of running the cyclo-depolymerization reaction at lower temperature, thus saving energy. Moreover, this solvent has high production volumes due to its widespread use as solvent mainly for polymerization reactions [62], [63]: this means immediate availability at cheaper price. From the environmental point of view, DSMO would be the best option since it is classified as non-toxic for human being and for environment.

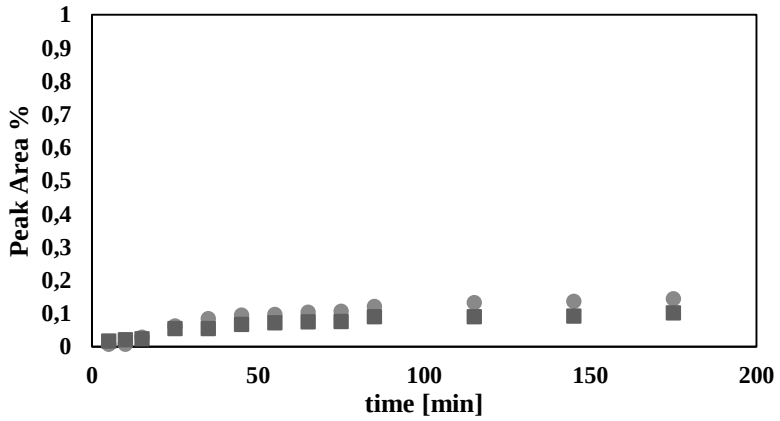

Figure 4.4.4 Cyclodepolymerization reactions in DMSO at prepolymer concentration of 10g/L without catalyst and different temperatures: 170°C (●) and 130°C (■).

Reactions in DMSO were run at different temperatures (Figure 4.4.4): surprisingly, the final yield in terms of cyclics was very low and about 10% after 3h. To speed up the approach to equilibrium conversion, a catalyst (dibutyltin oxide) was added to the solution in large amount (Figure 4.4.5). Even at the highest examined temperature, the final yield was only slightly above 20%.

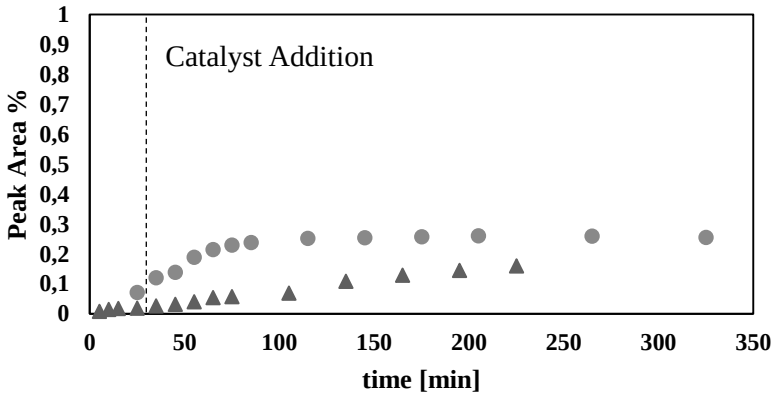

Figure 4.4.5 Cyclodepolymerization reactions in DMSO at prepolymer concentration of 10g/L with catalyst and different temperatures: 170°C (●) and 130°C (▲).

This phenomenon can be partly explained by considering the high hygroscopicity of the solvent, which could lead to quite intense hydrolysis of the product (cf. Figure 4.4.6). Hydrolysis reactions compete with cyclization reactions degrading the linear chains needed for ring closure, thus reducing the final yield of the reaction.

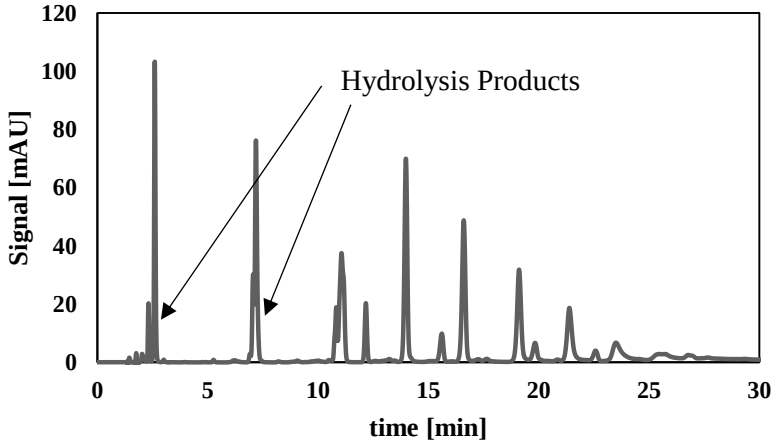

Figure 4.4.6 HPLC plot of a cyclodepolymerization reaction in DMSO at 170ºC after 3 hours.

The role of the solvent is fundamental in cyclization reaction since the affinity of the linear chains to the solvent results in different spatial conformation of the molecules. If the linear pre-polymer has high affinity to the solvent, the chain would be stretched thus lowering the probability of closing on itself; on the other hand, a bad solvent with lower affinity would result in a coil conformation, thus increasing the probability of chain closure. This concept is also

accounted for in the mathematical model developed by Jacobson and Stockmayer through the term related to the end-to-end distance. The larger the distance, the smaller the probability of cyclization becomes. When considering the effect of the solvent on reaction equilibrium, negligible enthalpic contribution is expected, since differences in solvation energy between cyclics and linear chains are negligible. On the other hand, the solvent quality can have a significant effect on the entropic term if the polymer solution is diluted and the solvent is good, since the chain becomes expanded and the probability of chain end closure falls dramatically [47].

To conclude, the feasible alternatives to 2-methylnaphthalene are:

(i) diphenyl ether that showed comparable results to the previous solvent with the advantage of an easier handling of the solvent;
(ii) dichlorobenzene that can be exploited at lower temperature, providing high purity of the final product, thus facilitating the purification step;
(iii) dimethyl sulfoxide which enables lower reaction temperature, thus saving energy and reducing the environmental impact of the process.

4.5 Application of the Jacobson and Stockmayer (J&S) model to cyclodepolymerization reactions

In order to design a process aiming to a specific amount of cycles, the thermodynamics of the system needs to be well understood: cyclodepolymerization reactions were then carried out to obtain enough experimental data in order to measure reaction kinetics and cyclic yield at equilibrium. Reaction conditions were maintained constant: temperature of 200 ºC, no catalyst, 2-methylnaphthalene as solvent and three hours of reaction. Different initial concentrations of prepolymer were considered: 5, 10 and 20 g/L. Each experiment was repeated at least three times to ensure reproducible data.

The aim of the J&S model is to predict the final equilibrium mass of cyclic species and their distribution as a function of the amount and the composition of the prepolymer charged, temperature, and type of solvent.

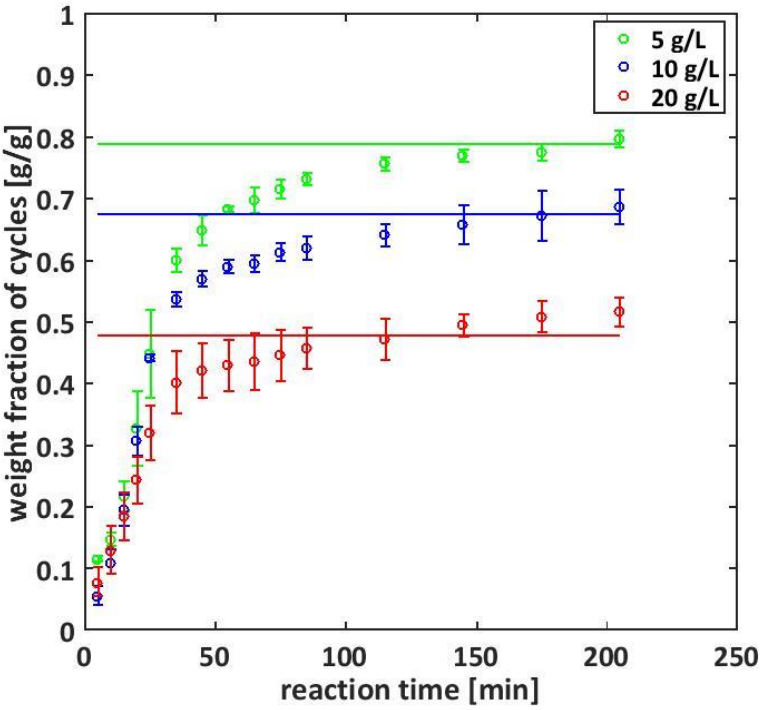

Figure 4.5.1 Time evolution of the weight fraction of cyclic oligomers with respect to (cyclic + linear) species: solid lines represent the equilibrium values predicted through the J&S model. The experimental data correspond to different initial concentrations of prepolymer: 20 g/L (red), 10 g/L (blue), 5 g/L (green).

In Figure 4.5.1, the kinetic evolutions of the experimental weight fraction of cyclic oligomers at three different initial concentrations of prepolymer are shown and compared with the

equilibrium values predicted by J&S model (the same values are also shown in Table 4.5.1). The agreement between model predictions and experimental data is quite good.

Table 4.5.1 Weight fractions at equilibrium predicted by the model and measured experimentally.

	Weight fraction of cycles [g/g]	
Prepolymer Concentration [g/L]	**Experimental**	**Predicted**
5	0.517	0.5647
10	0.683	0.7223
20	0.797	0.8133

Additionally, the complete distributions of chain length and ring size are compared with the model predictions in Figure 4.5.2: again, the agreement between model and experiments is satisfactory.

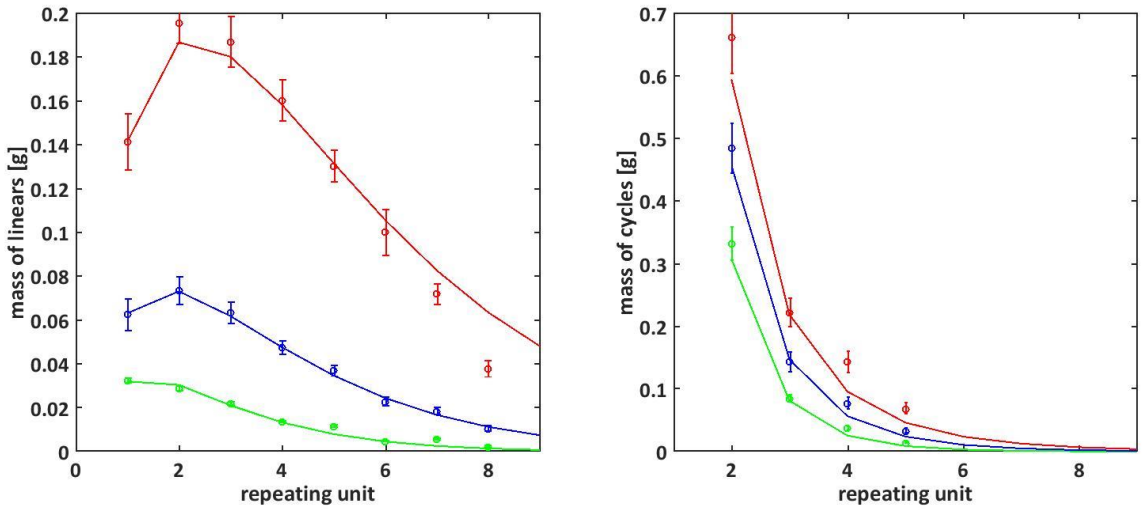

Figure 4.5.2 Final distributions of linear (left) and cyclic (right) with different repeating units predicted by the model (solid line) together with the averaged experimental data referred to different concentrations: 20 g/L (red), 10 g/L (blue), 5 g/L (green).

The used model parameter values (equilibrium constants) are summarized in Table 4.5.2 and compared to those estimated in the case of dichlorobenzene in a previous Master Thesis [34].

The effective bond length is slightly larger in the case under examination, thus explaining the lower purity of the cycles produced in 2-MN compared to those produced in DCB. As shown in the table, the difference between the two cases is associated to the larger stiffness of the linear chains in 2-MN, thus confirming that solvent quality affects the reaction yield at very significant extent.

Table 4.5.2 Summary of model parameters: K_c, equilibrium constant for step growth, K_1, equilibrium constant referred to unitary linear chain and b, chain stiffness.

	K_c	K_1	b [A]
2-methylnaphthalene	0.50	1.25	3.60
Dichlorobenzene [34]	0.50	1.47	3.25

4.5.1 Model improvements

In the J&S model, the equilibrium constant of global Ring Chain Equilibrium, $K_{J\&S}$, depends on the length *n*, cf. Eq. 3.16. The effective chain length *b*, can be directly related to the mean square end-to-end distance of a random flight chain of *n* units. J&S theory requires a reliable value of *b* in order to predict accurately the equilibrium constant.

One possible model improvement would be represented by the use of the Rotational Isomeric State (RIS) model to predict the end-to-end distance of the linear chains. In fact, the representation of the spatial configuration of macromolecules based on RIS theory has been proved to be an effective tool [64]. Indeed, the estimation of $K_{J\&S}$ combining J&S and RIS theories provide values that agree very well with the experimental data for macrocyclics (more than 30-40 backbone atoms) while, for smaller cycles, predicted equilibrium constants are not accurate [47]. This discrepancy between J&S-RIS model and experiments could have an enthalpic origin. In fact, if a ring has less than 20-30 backbone atoms, there generally exists a strain energy, that can significantly affect ring-chain equilibrium constants. In ring chain equilibria the enthalpic change is due only to strain energy, since the bond energy is unchanged in the corresponding reaction and intermolecular interactions are barely changed. Ring strain becomes negligible only for molecules that contains 100 atoms or more, so rings have to be large enough to be strain free [13]. Ring strain energy is significant for small rings of up to about 20 backbone atoms.

Thus, another improvement could be considering an enthalpic change due to cyclization reaction; this way, prediction of equilibrium constants would be more precise.

4.6 Selective Precipitation: influence of temperature on the final purity

The first studied purification method was precipitation, justified by the fact that cyclic species have different solubility with respect to linear chains. After depolymerization, the system was cooled down at different temperatures and the precipitation was monitored by measuring the evolution of the concentrations in the liquid phase for 1.5 h, as shown in Figure 4.6.1.

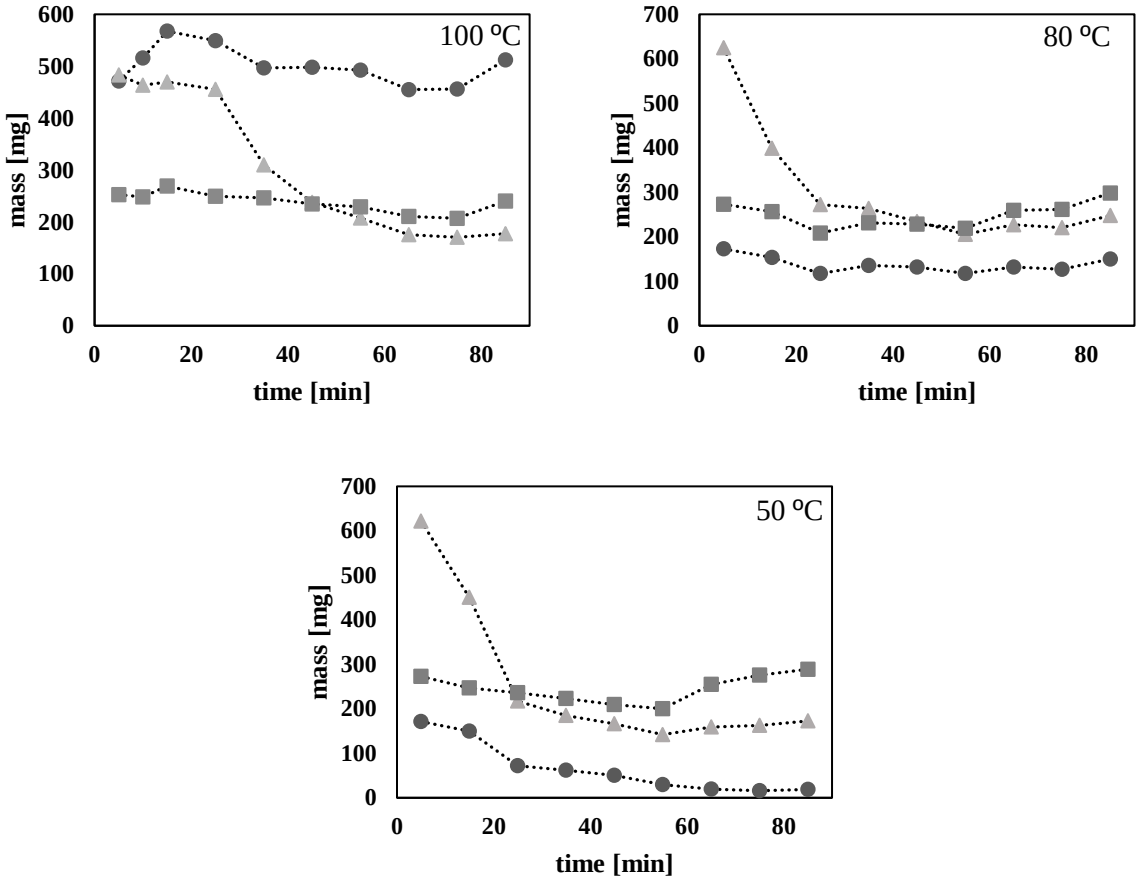

Figure 4.6.1 Liquid phase compositions at different temperatures during precipitation experiments: cycle C2 (▲), bigger cycles C3, C4, C5, C7 (■) and linear chains (●).

Decreasing the temperature, the cyclic dimers are the species precipitated at the largest extent, followed by the linear chains at the lowest temperature. Therefore, a careful selection of temperature is crucial for this process step to control the purity of the recovered cyclic oligomers. Such purity has been defined as:

$$Purity = \frac{\left(m^{initial} - m^{final}\right)_{cycles}}{\left(m^{initial} - m^{final}\right)_{cycles} + \left(m^{initial} - m^{final}\right)_{linears}}$$

and the values for the three experiments mentioned above are summarized Table 4.6.1.

Table 4.6.1 Purity of precipitation experiment as a function of temperature

Precipitation Temperature [ºC]	**Purity (cyclic mass %)**
100	90.36
80	75.98
50	73.94

The best operating temperature is around 100 ºC, while lower temperatures showed lower purity. It is interesting to note that 100 ºC is a critical value of temperature below which precipitation becomes almost nonselective. Note that, even though the purity has been defined with respect to cycles of ant size, the solid product is mainly made of the cyclic dimer.

To summarize, the main advantage of selective precipitation is its relative simplicity. On the other hand, achievable purification is not enough for ring opening polymerization and recycling of unreacted products is difficult because the linear species precipitated together with cyclics need to be removed via selective adsorption on Si-gel.

4.7 Selective Adsorption on Zeolites

As alternative purification method, selective adsorption was explored using a solid adsorbent. In previous studies, Si-gel was exploited for this goal [33], [34] and very high purity could be achieved. The final solid product consisting of a mixture of cyclic and linear species was dissolved in 7.5 v/v% DEE/DCM solvent mixture and purified using a column packed with Si-gel. The weakness of this method was the low productivity 800 mg/14 L [33] and the necessity of using a solvent different from the one used during the reaction, thus involving an expensive solvent exchange. Therefore, different adsorbents (zeolites) have been considered in this work, able to purify the final product without any solvent exchange.

4.7.1 Adsorption at room temperature

The first screening study was performed at room temperature to quickly evaluate the adsorption selectivity between linear and cyclic species for different adsorbents. Four different zeolites, whose properties are summarized in Table 4.7.1, were examined.

Table 4.7.1 Main properties of the different zeolites

	CBV 790	**BETA H**	**HSZ 890**	**HSZ 390**
SiO_2/Al_2O_3 mole ratio	80	500	1500	500
Na_2O weight %	0.03	<0.05	<0.05	0.05
Unit cell size [Å]	24.24	n/a	n/a	24.5
Surface Area [m^2/g]	780	500	310	630

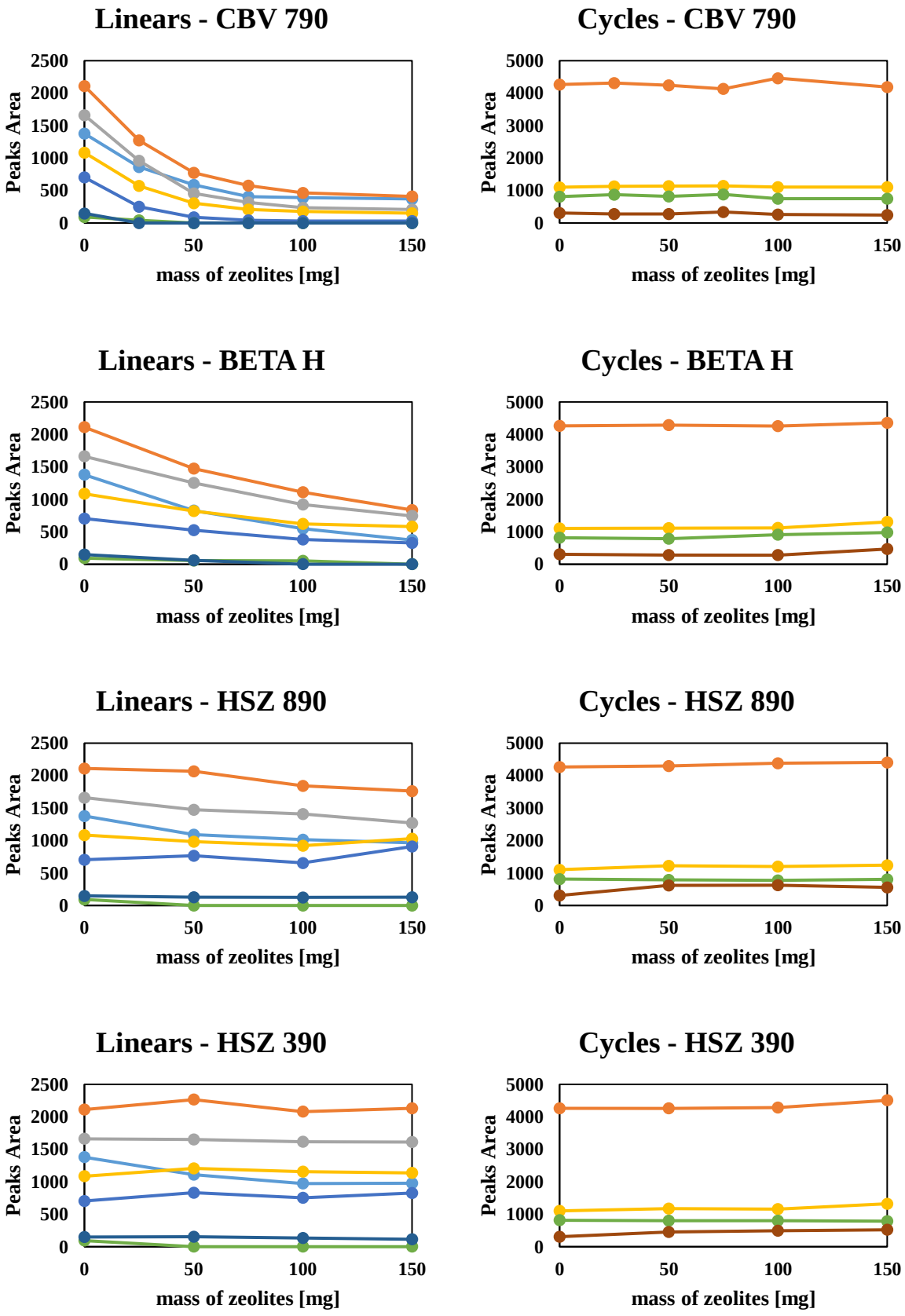

Figure 4.7.1 Zeolite screening: peak area of different species vs. mass of adsorbent. Linears: L1 (●) L2 (●) L3 (●) L4 (●) L5 (●) L6 (●) L7 (●). Cycles: C2 (●) C3 (●) C4 (●) C5 (●)

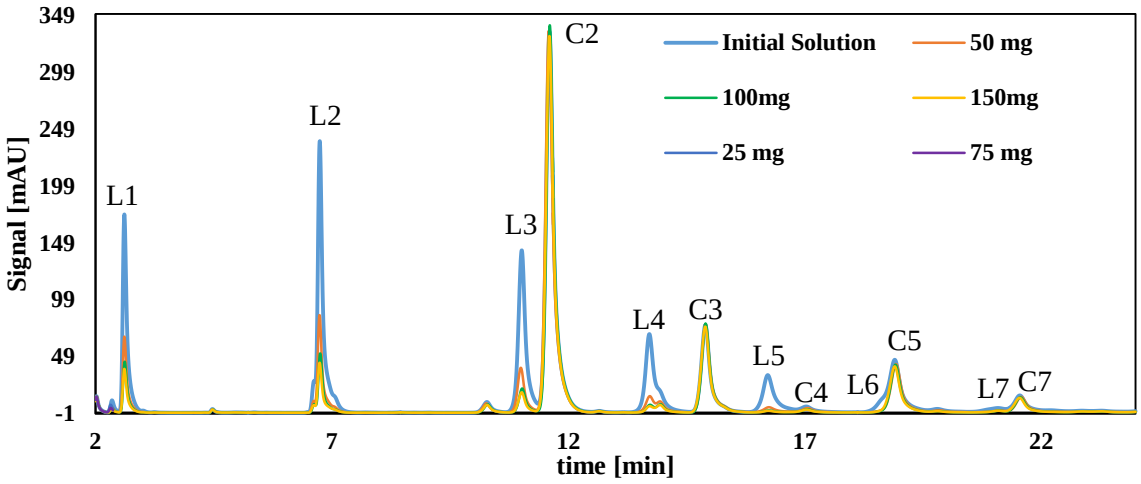

Figure 4.7.2 HPLC trace showing that peak areas associated to cyclic species maintained their height even after adsorption while linear peak areas are selectively reduced

As shown in Figure 4.7.1, linear and cyclic species behave differently with different adsorbents. The first two zeolites, zeolite Y (CBV 790) and zeolite beta (BETA H), showed a clear selectivity towards linear species. Peak areas of linear are decreasing increasing the amount of adsorbent, while cyclic species remained almost unaffected. In case of zeolite Y (CBV 790) the selectivity is the same but the loading capacity seems higher, since the peak areas of the single linear species for 150 mg of adsorbent decrease to less than 500 [mAU] (milli-Abs Units), while for zeolite beta the reduction is less (down to about 1000 [mAU]). On the other hand, the last two zeolites, zeolite ZSM-5 (HSZ 890) and zeolite Y (HSZ 390), do not exhibit any significant selectivity: only the shortest, linear chains, L1 and L2, are adsorbed in very small amount. It is interesting to notice that the different behavior of the two zeolites Y could be due to their different composition, namely in terms of SiO_2/Al_2O_3 molar ratio, a quantity determining the solid acidity. The number of cations in the crystal cages depends on Si to Al ratio: each Al atom brings one negative charge to be compensated by adequate number of mono- or multivalent cations. This ratio affects the adsorptive properties of zeolite [65] and larger values of the Si:Al ratio resulted in higher selectivity.

For the specific case of zeolite Y (CBV 790), the selective adsorption of the linear species is well visualized in Figure 4.7.2. The initial solution (light blue line) is composed by a mixture of linear and cyclic species: immediately after the addition of zeolite, the peaks corresponding to the shortest linear chains (repeating units from 1 to 4) are strongly reduced, while those corresponding to longer linear chains disappear completely. At the same time, the peak areas

associated to cyclic species remained practically constant, thus confirming very high adsorption selectivity.

4.7.2 Adsorption at reaction temperature

Once identified an adsorbent with high enough selectivity towards linear species, the adsorption experiments have been repeated at the reaction temperature. Since it is well known that zeolites can act as reaction catalysts, especially at high temperatures [49] [53] [66], their possible effect on the cyclization reactions was considered. In order to decouple reaction and adsorption, the zeolites were added after equilibration of the depolymerization reaction and no further reaction was ongoing. Since the equilibration time of the reaction was estimated around 3h from previous experiments, given amounts of zeolite Y (CBV 790) were directly charged to the reactor after this time. These adsorption experiments were carried out using 2-MN as solvent, the favorite reaction medium considered in all pilot plant experiments producing cyclic oligomers.

In the first adsorption experiment, zeolites were used without any pretreatment. Contrarily to adsorption at room temperature, the high reaction temperature promoted hydrolysis reactions most probably due to the water originally present in the zeolite. For this reason, the zeolites for further experiments were invariably calcined at 400 ºC and stored under inert atmosphere prior to usage.

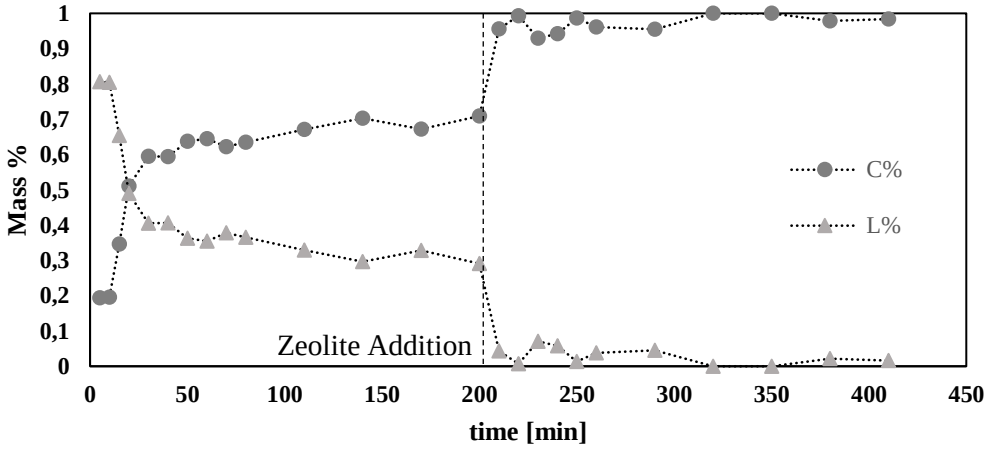

Figure 4.7.3 Time evolution of linear and cyclic species. Mass percentage of cyclics is dramatically increased after addition of the adsorbent medium.

The time evolutions of the mass percentage of the two groups of species involved in the equilibrium are shown in Figure 4.7.3. The initial reaction followed the typical trend of cyclodepolymerization, consisting in the first dissolution interval at increasing temperature followed by reaction equilibration. After more than 3h, zeolite was added and the solid-liquid contact was maintained for three more hours. Right after the zeolite addition, the mass percentage of linears decreased very rapidly to values smaller than 10% in 10 minutes, reaching even lower values after short time. Accordingly, the cyclic species in the liquid phase reached very high purity while the majority of the linear species were retained in the solid phase.

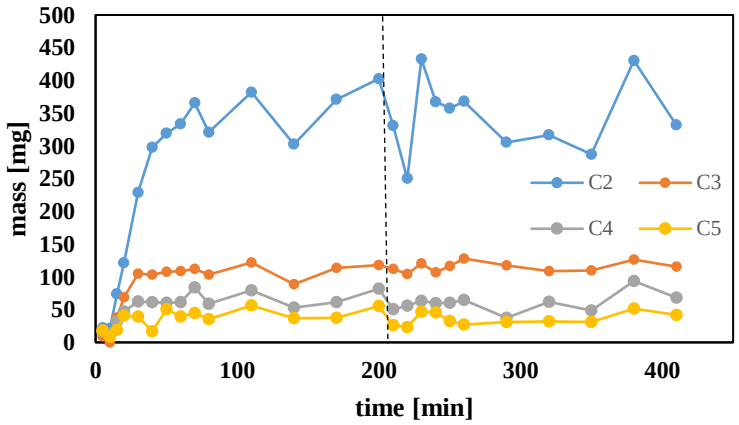

Figure 4.7.4 Mass evolution of the single cyclic species during the experiment. Dashed line define the zeolite addition

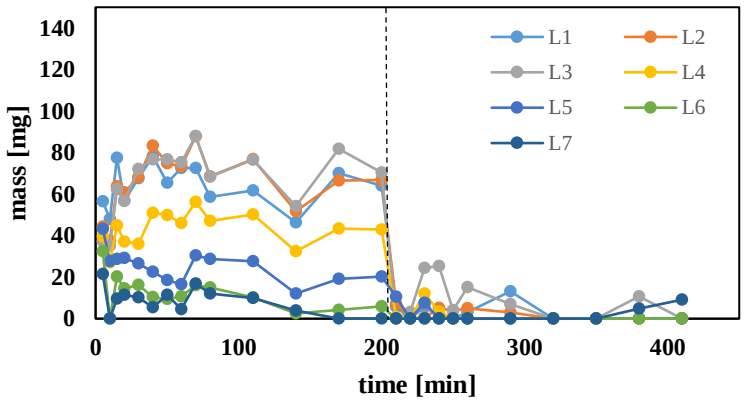

Figure 4.7.5 Mass evolution of the single linear species during the experiment. Dashed line define the zeolite addition

In Figure 4.7.4 and Figure 4.7.5, the time evolutions of the amount in the liquid phase of each single species are shown. While the complete adsorption of the linear oligomers is confirmed even at high temperature, the complete exclusion of the cyclic oligomers from the solid is clear. The only species partly interacting with the adsorbent is the smallest cycle, C2. Some scattering in the measured amount of C2 is apparent: the reason of such scattering is not clear and should be due to measurement error. Note that the reaction is fully prevented after adsorption: in fact, both the linear species and EG are fully adsorbed and the cyclic oligomers alone cannot back-react to form linear chains. The loading capacity of zeolite Y (CBV 790) is very large, corresponding to adsorbed amount close to 27% by weight. Moreover, the adsorption kinetics is very fast, most probably due to the powder-form of the adsorbent, with very small particle size (~10 microns).

4.7.3 Batch adsorption studies at reaction temperature

In order to analyze the adsorption behavior in a more systematic way, adsorption experiments were performed at reaction temperature and different amounts of zeolite. This way, the optimal zeolite to prepolymer ratio and the loading capacity could be evaluated. These experiments were carried out using the same protocol described in the previous paragraph.

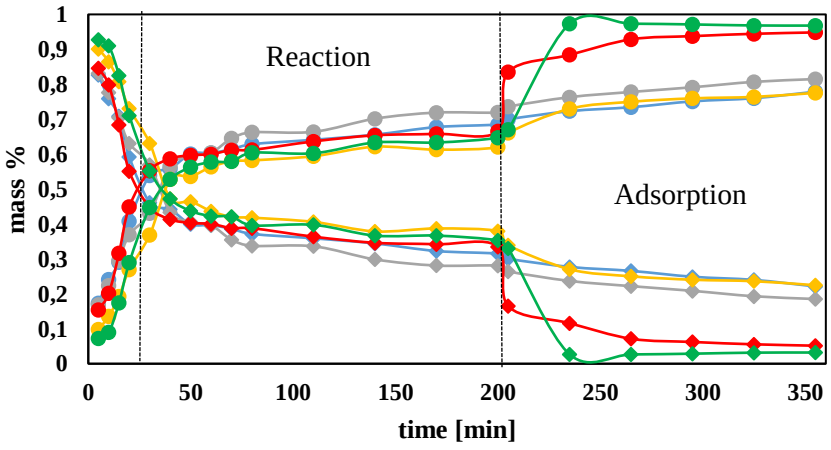

Figure 4.7.6 Five different adsorption experiments after equilibration at reaction temperature. Zeolite amount: 2g (green), 1g (red), 0.5g (yellow), 0.2g (grey) and 0.1g (blue) linear (♦) and cyclic (●) species.

Table 4.7.2 Purity is function of the amount of zeolites added to the system, the values showed in the table refers to the purity achievable after 1 hour of adsorption at reaction temperature

Zeolite Mass [mg]	**100**	**200**	**500**	**1000**	**2000**
Purity %	77,8	82,6	78,6	94,8	96,8

As shown in Figure 4.7.6, the purity of the final product is increasing at increasing solid holdup. In particular, the adsorption of linear oligomers is almost complete at the largest amount of solid (2g), from which the loading capacity of the adsorbent can be estimated.

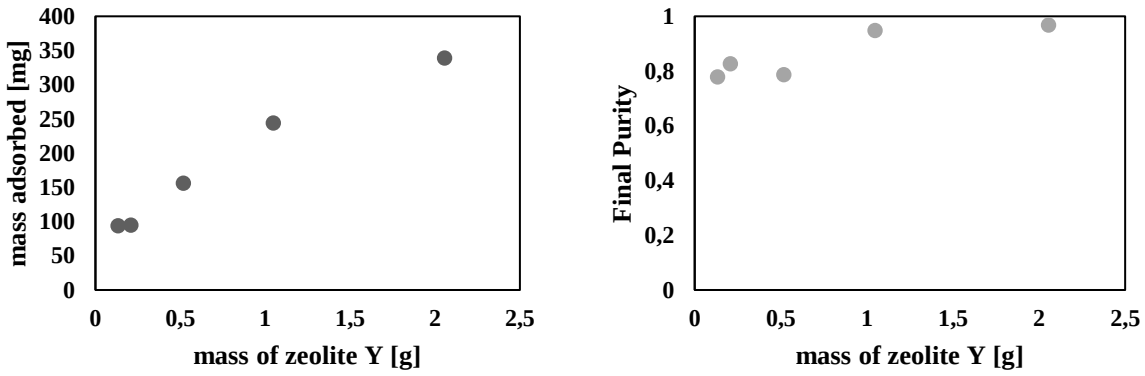

Figure 4.7.7 Mass of species adsorbed increases with the amount of adsorbent employed (left graph). Cycles purity reached at equilibrium: even with small amount of adsorbent purity is close to 80% while, by adding 1g of adsorbent it is around 94,8%.

Given the multicomponent nature of the system under examination, an effective adsorption isotherm was expressed lumping together all linears oligomers. With this aim, the five experiments, whose results are summarized in Figure 4.7.8 as time evolution of the concentration in liquid phase, were carried out.

I)

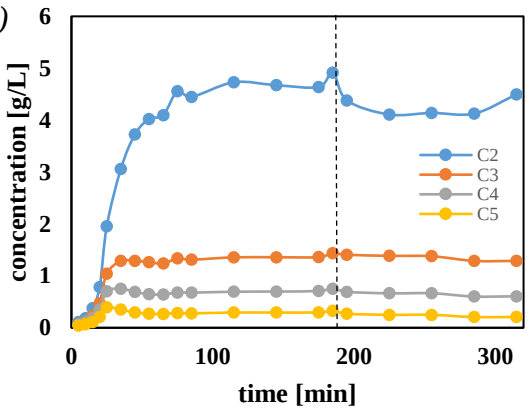
concentration [g/L]
time [min]
C2
C3
C4
C5

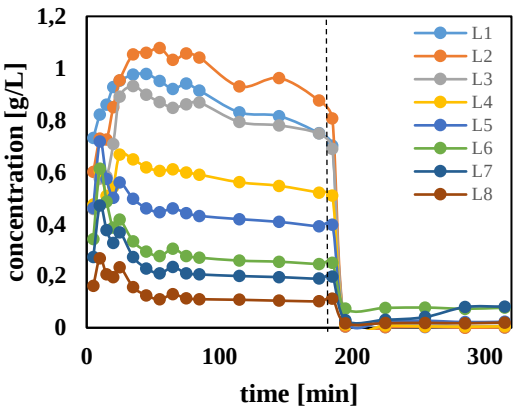
concentration [g/L]
time [min]
L1
L2
L3
L4
L5
L6
L7
L8

II)

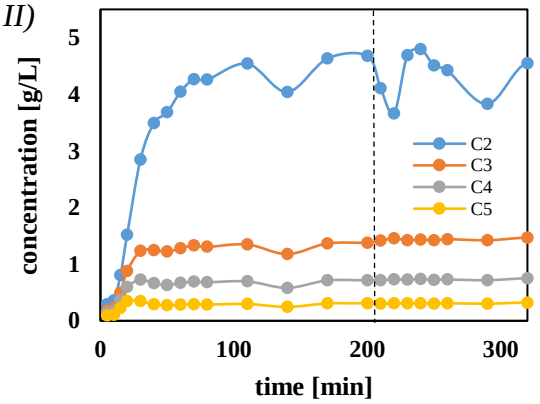
concentration [g/L]
time [min]
C2
C3
C4
C5

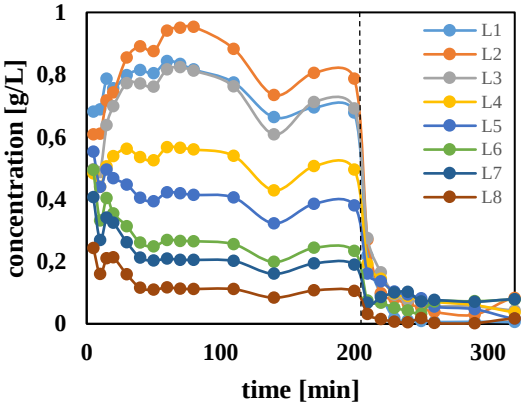
concentration [g/L]
time [min]
L1
L2
L3
L4
L5
L6
L7
L8

III)

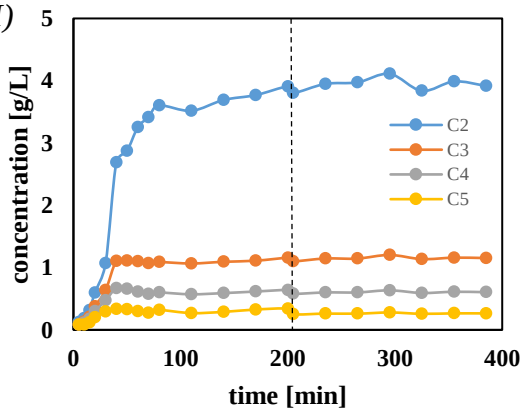
concentration [g/L]
time [min]
C2
C3
C4
C5

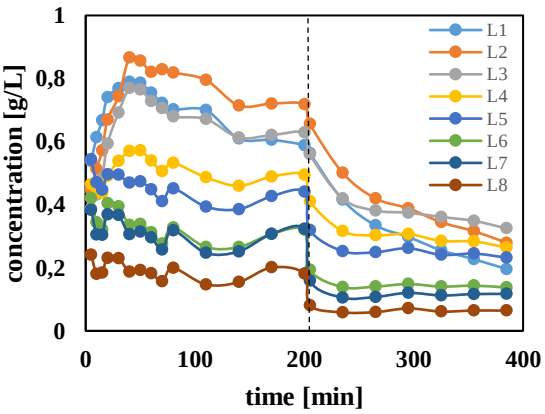
concentration [g/L]
time [min]
L1
L2
L3
L4
L5
L6
L7
L8

IV)

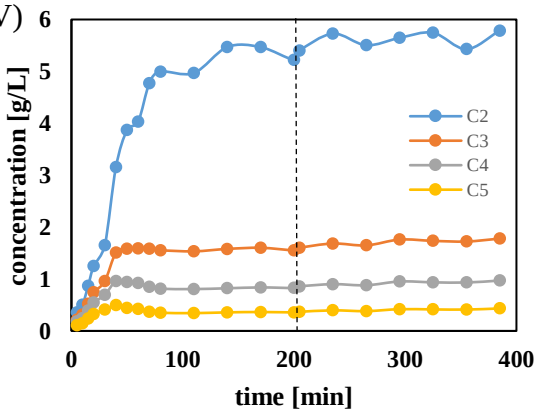
concentration [g/L]
time [min]
C2
C3
C4
C5

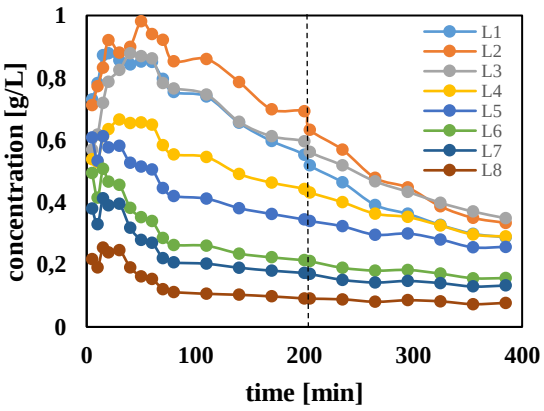
concentration [g/L]
time [min]
L1
L2
L3
L4
L5
L6
L7
L8

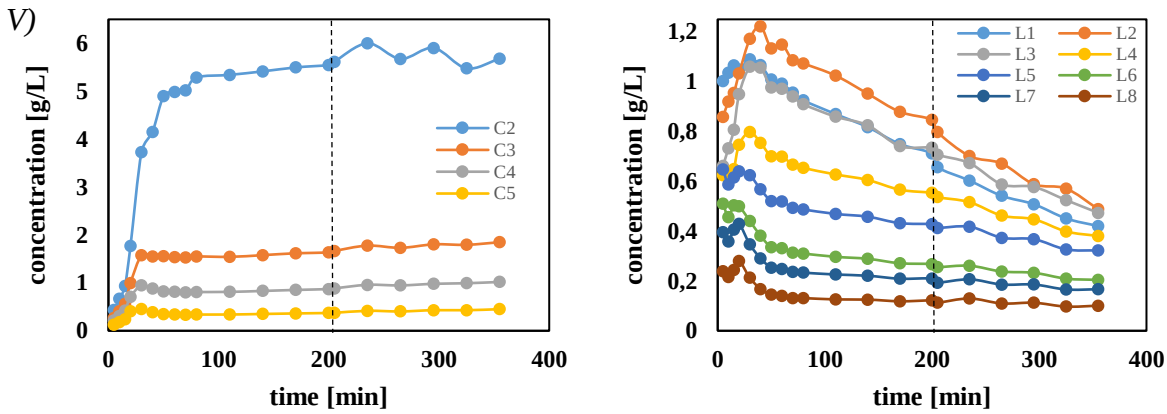

Figure 4.7.8 Cyclics and linears evolution in time per different amounts of zeolites added to the system: I) 2g, II) 1g, III) 0.5g, IV) 0.2g, V) 0.1g. Dashed line divides reaction time from adsorption time, corresponding to that time zeolites were added. Every species with its characteristic length is associated to the number of repeating units in it.

Note that equilibrium conditions were assumed to be established after 10 min after zeolite addition: this contact time was assumed to be large enough to achieve adsorption equilibrium and short enough to have negligible extent of reaction in the liquid phase. When considering small amount of adsorbent, a limited reduction in linear species is found; therefore, the linear species remaining in the liquid phase could further react (and they do, as indicated by their decreasing concentrations at long time). On the other hand, when large zeolite amounts are used, the linear species are fully removed from the liquid phase, thus quenching the reaction. This behavior is consistent with the reaction scheme considered in Chapter 3.

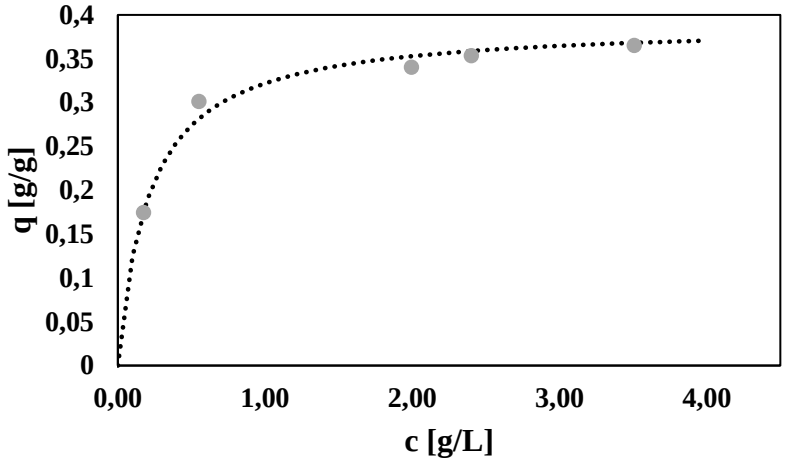

Figure 4.7.9 Adsorption Isotherm showing the loading capacity q as a function of adsorbent concentration c.

The estimated adsorption isotherm of the linear species is reported in Figure 4.7.9. Langmuir type behavior isotherm could be reasonably well fitted to the experimental data.

These results are quite promising in view of the development of a purification process based on adsorption. On the other hand, the recovery of the adsorbed linear species is crucial in order to recycle such components to the depolymerization reactor and ensure high cyclic yields. Therefore, the desorption behavior is quickly examined in the following section.

4.8 Desorption

Given the large affinity of the linear species for the adsorbent and the high operating temperature, the use of a liquid solvent suitable to "displace" the adsorbed species is the most promising approach to be considered. Even though the operating temperature of the adsorption measurements was the same as the reaction temperature, desorption experiments at room temperature were initially performed.

4.8.1 Desorption at room temperature

After an adsorption experiment at room temperature, the equilibrated solid was packed into a column and "washed" with 1L of a solvent mixture DCM/MeOH. The collected liquid phase was then analyzed to evaluate nature and amount of the desorbed components.

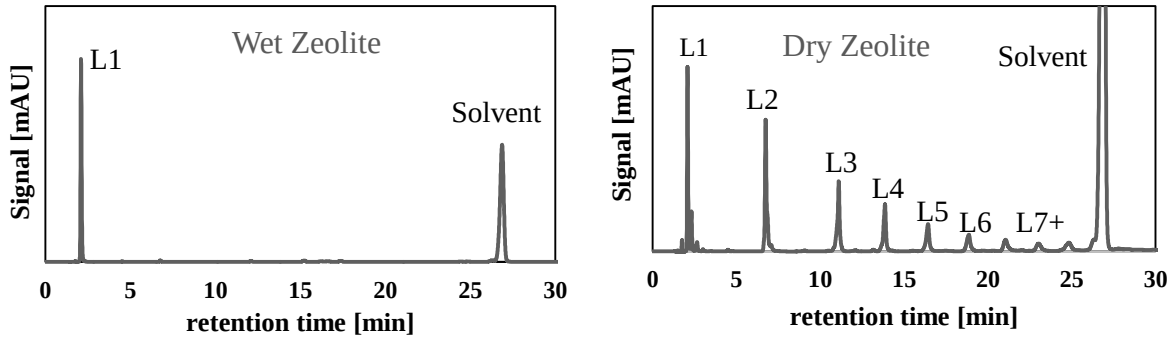

Figure 4.8.1 HPLC traces of two desorption experiment on zeolites. On the left untreated zeolite, on the right zeolite dried in vacuum oven at 110°C.

In Figure 4.8.1, the HPLC traces corresponding to the collected desorption products using untreated and calcined zeolites. While a single peak (the shortest linear oligomer, L1) appears in the case of untreated zeolites, all linear oligomers are recovered when using calcined zeolites. These results further confirm that the use of untreated zeolites induces the complete degradation of the desorbed linear chains. Zeolites are indeed hygroscopic materials able to retain moisture from air, which is enough to promote hydrolysis reactions.

The selected binary solvent (DCM/MeOH) was effective to achieve almost complete desorption at room temperature, verified by closing the mass balance on the initial prepolymer used for

cyclodepolymerization and subsequent adsorption. The desorbed mixture is made of linear oligomers only, thus confirming the negligible adsorptivity of the cyclic oligomers. On the other hand, 1L of solvent mixture is needed to regenerate 1g of solid zeolites: such huge ratio desorbent to adsorbent is indeed unrealistic in view of the industrial application.

4.8.2 Desorption at high temperature

As anticipated, the best option for an integrated process combining reaction and adsorption would be to have the same solvent for both steps. Therefore, all the solvents previously studied for the reaction step were further screened as possible displacement agents.

Table 4.8.1 Summary of desorption conditions.

Solvent	T [°C]	V [mL]	Zeolite amount [g]
2-MN	200	100	1
DPhE	200	100	2
DCB	180	100	2
DMSO	150	100	2

Few standard experiments of reaction in 2-MN followed by adsorption were done and after three hours of reaction, zeolites were collected by hot filtration in order to avoid as much as possible cycle precipitation on them. Subsequently they were put in a glass reactor with fresh solvent and heated up.

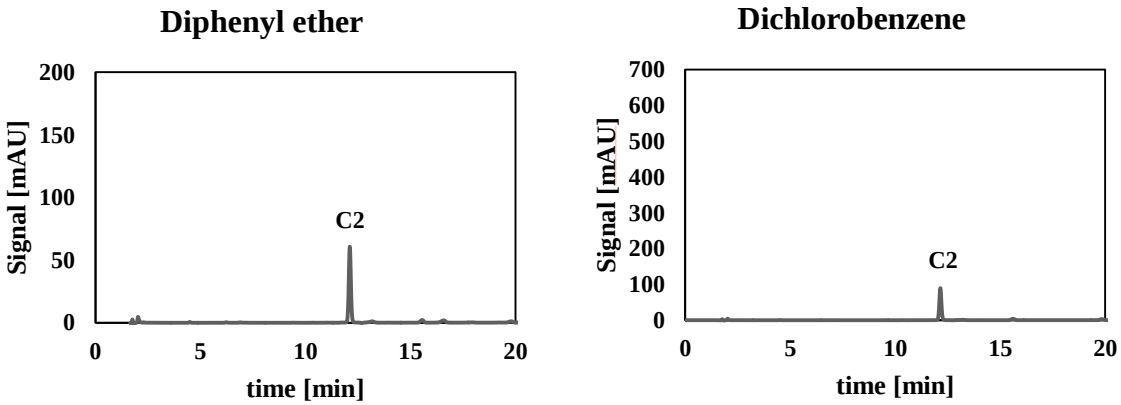

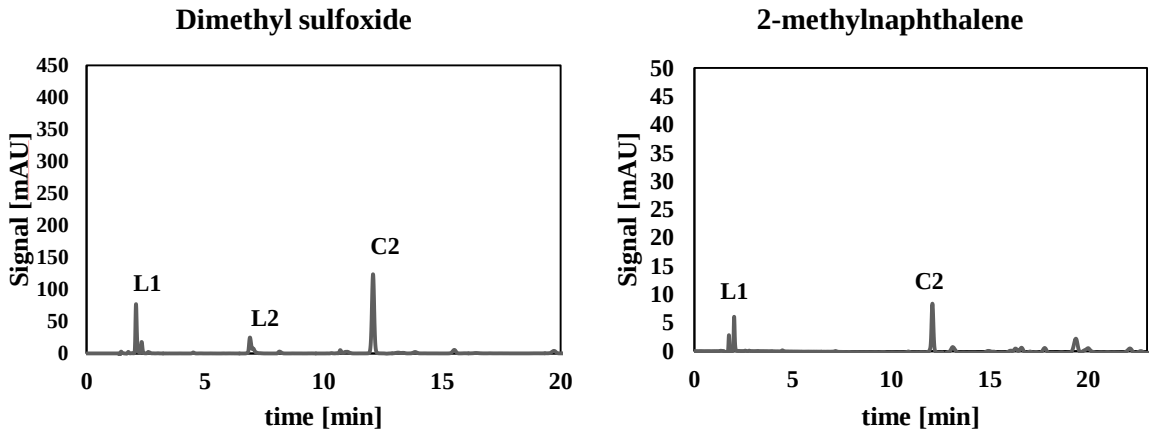

Figure 4.8.2 HPLC signals of four desorption experiments after three hours of reaction.

Desorption experiments at high temperature were not able to desorb any linear species, a part from dimethyl sulfoxide which desorbed few short linear chains. In each cases peak corresponding to cycle with repeating unit two is present, this can be explained considering the difficulties in handling 2-methylnaphthalene as solvent: C2 cycles are dissolved in the liquid phase but, during hot filtration, a certain amount of solvent was retained on the zeolite themselves. Thus in desorption experiments, high temperature melted the residual solvent releasing cycles into the liquid phase.

To conclude, desorption was successful only using DCM/MeOH mixture at room temperature, while for the other cases only dimethyl sulfoxide was able to desorb linear chains. Adsorption on zeolite Y (CBV 790) seemed also almost irreversible. Nevertheless, it could also have been the case that the desorbed linears in all the cases would have reequilibrated to cyclic oligomers.

5 Conclusions and Outlook

The possibility of exploiting cyclodepolymerization reaction for the production of cyclic oligo-(ethylene furanoate) was explored in this work, considering both reaction and the following purification.

Taking advantage of suitable calibration, the reaction yield was carefully quantified by HPLC. The final amount of cyclic oligomers produced through cyclodepolymerization reaction carried out in 2-methylnaphthalene at about 200°C was about 50% of the initial prepolymer mass (500 mg out of an initial mass of 1g of prepolymer).

All the experimental data collected by HPCL were used to validate a mathematical model which has been developed based on Jacobson and Stockmayer theory. The model predictions agree very well with the experimental data at reaction equilibrium in terms of overall yield as well as entire size distribution of the different species. Through the model, kinetic parameters and chain stiffness were estimated.

An important aspect of the process design is represented by the selection of a suitable solvent, whose impact on the final reaction yield is crucial. Starting from a solvent previously applied for the same reaction (2-methylnaphthalene), alternative solvents have been considered, namely diphenyl ether, dichlorobenzene and dimethyl sulfoxide. Diphenyl ether showed performance comparable to that of 2-MN; on the other hand, dichlorobenzene resulted to be a poor solvent, even though higher yield could be achieved in this case. Other potential solvents (e.g. p-xylene) could not be considered because of the required pressurized reactor: they will be subject of future work focused on the development of more sustainable process.

Finally, a novel purification method for the produced cyclic oligomers (high purity is essential for the following polymerization step) based on adsorption was explored. Selective adsorption was successfully applied using zeolite as adsorbents. A crucial parameter controlling the adsorption behavior is the adsorbent acidity, which is the silica to alumina ratio in the solid matrix. The highest purity (~96%) was obtained by combining standard reaction in 2-methylnaphthalene with the use of zeolite Y (CBV 790) in powder form. A direct relationship between the amount of adsorbent species and the amount of adsorbent was reported, describing the equilibrium adsorption of the linear oligomers by the Langmuir Isotherm. When tuning properly the amount of adsorbent, the residual non-adsorbed linear species underwent cyclization reaction, increasing the yield of reaction. Solid regeneration with complete

desorption of the adsorbed components was possible by using a mixture of DCM/MeOH at room temperature.

These results constitute the basis towards the development of a process integrating reaction and purification aimed to produce cyclic oligomers suitable for the following ring-opening polymerization step. In particular, further efforts are needed to identify the right match of solvent-adsorbent able to selective adsorb and subsequently desorb linear species, thus enhancing the reaction yield together with the product purity.

Appendix:

Appendix 1: Table of Calibration Curves

	Calibration curve 1		Calibration curve 2		Calibration curve 3	
%v/v	Peak Area	Concentration [g_{2MN} / g_{GPCS}]	Peak Area	Concentration [g_{2MN} / g_{GPCS}]	Peak Area	Concentration [g_{2MN} / g_{GPCS}]
0	0	0	0	0	0	0
1:20	83802.0781	0.009621143	84678	0.006163762	74432.7266	0.007837353
1:10	106420.086	0.016465054	111641.477	0.013013335	111247.031	0.018769576
1:5	138663.594	0.031426133	141768.688	0.03064713	137333.688	0.038269427
1:2	191687.313	0.102468434	197446.656	0.089078041	179714.344	0.099220607
1	235828.484	0.215579645	240167.188	0.212111069	223635.063	0.219336569

	Calibration curve 1		Calibration curve 2		Calibration curve 3	
%v/v	1/ $A^{2.79}$	1/ C_{2MN}	1/ $A^{2.79}$	1/ C_{2MN}	1/ $A^{2.79}$	1/ C_{2MN}
0	0	0	0	0	0	0
1:20	1.83704E-14	103.93775	1.78451E-14	162.23859	2.55728E-14	127.59411
1:10	9.43201E-15	60.734692	8.25214E-15	76.844251	8.33403E-15	53.277708
1:5	4.50739E-15	31.820651	4.23732E-15	32.629483	4.63022E-15	26.130519
1:2	1.82627E-15	9.759103	1.68149E-15	11.226111	2.18632E-15	10.078552
1	1.02437E-15	4.6386569	9.73569E-16	4.7145111	1.18791E-15	4.5592033

Appendix 2: summary of cyclo-depolymerization reactions

Reaction	Solvent	Concentration [g/L]	T [ºC]	Catalyst	Comments
1	2-methylnaphthalene	10	200	Dibutyltin oxide	GPC analysis Precipitation 50 ºC
2	2-methylnaphthalene	10	200	Cystox	GPC analysis
3	2-methylnaphthalene	10	200	Titanium isopropoxide	GPC analysis
4	2-methylnaphthalene	10	200	Cystox.	Prepolymer synthetized previously [33] GPC analysis
5	2-methylnaphthalene	10	200	Four times cystox amount.	Prepolymer synthetized

					previously [33]
6	2-methylnaphthalene	10	200	Cystox	GPC analysis GPC analysis
7	2-methylnaphthalene	10	220	Cystox	GPC analysis Precipitation 100ºC
8	2-methylnaphthalene	10	200	Cystox	GPC analysis Precipitation at 100ºC
9	2-methylnaphthalene	10	200	KCl salt added	GPC analysis
10	2-methylnaphthalene	10	200	Cystox	Precipitation 90 ºC
11	2-methylnaphthalene	20	200	Cystox	Precipitation 90 ºC
12	2-methylnaphthalene	10	200	Cystox	Precipitation 90 ºC
13	2-methylnaphthalene	10	200	Cystox	Precipitation 50 ºC
14	Diphenyl ether	10	200	Cystox	
15	2-methylnaphthalene	10	200	No	. Addition of 1g of zeolite Y (CBV 780)
16	2-methylnaphthalene	10	200	Cystox	Prepolymer synthetized previously [33]
17	2-methylnaphthalene	10	200	Cystox	Precipitation 100ºC
18	2-methylnaphthalene	10	200	Cystox	Indirect calibration. Precipitation 100ºC
19	2-methylnaphthalene	10	200	Cystox	Indirect calibration. Precipitation 80 ºC
20	2-methylnaphthalene	10	200	Dibutyltin oxide	Indirect calibration. Precipitation 80 ºC
21	2-methylnaphthalene	10	200	Dibutyltin oxide	Prepolymer dried at 200ºC for 24 h. Indirect calibration.
22	2-methylnaphthalene	10	200	Twice amount of dibutyltin oxide	Indirect calibration.
23	Diphenyl ether	10	200	Dibutyltin oxide	Prepolymer dried at 200ºC for 24 h. Indirect calibration.
24	2-methylnaphthalene	10	200	No	Zeolite adsorption equilibrium. 1g of zeolite Y (CBV 780)
25	2-methylnaphthalene	5	200	Dibutyltin oxide	Indirect calibration. Precipitation 100ºC
26	2-methylnaphthalene	10	200	No	1g zeolite Y (CBV 780)
27	2-methylnaphthalene	10	200	No	1g zeolite Y (CBV 780)

28	2-methylnaphthalene	10	200	No	1g zeolite Y (CBV 780)
29	2-methylnaphthalene	5	200	Dibutyltin oxide	
30	2-methylnaphthalene	10	200	No	2g zeolite Y (CBV 780)
31	2-methylnaphthalene	10	200	No	0.1g zeolite Y (CBV 780)
32	2-methylnaphthalene	10	200	No	0.5g zeolite Y (CBV 780)
33	2-methylnaphthalene	10	200	No	0.2g zeolite Y (CBV 780)
34	2-methylnaphthalene	5	200	No	
35	2-methylnaphthalene	5	200	No	
36	2-methylnaphthalene	5	200	No	
37	2-methylnaphthalene	10	200	No	New synthetized prepolymer.
38	2-methylnaphthalene	20	200	No	New synthetized prepolymer.
39	2-methylnaphthalene	20	200	No	New synthetized prepolymer.
40	2-methylnaphthalene	20	200	No	New synthetized prepolymer.
41	Dichlorobenzene	10	190	No	
42	Dimethyl sulfoxide	10	150	No	
43	Dimethyl sulfoxide	10	170	No	
44	Dichlorobenzene	5	170	No	
45	Tetraethylene glycol dimethyl ether	10	200	No	
46	Dichlorobenzene	5	190	No	
47	Diphenyl ether	10	200	No	
48	Dichlorobenzene	5	200	No	
49	Diphenyl ether	5	200	No	
50	Dimethyl sulfoxide	10	130	No	
51	Dimethyl sulfoxide	10	130	Dibutyltin oxide	
52	Dimethyl sulfoxide	10	170	Dibutyltin oxide	
53	Diphenyl ether	10	200	No	
54	Diphenyl ether	10	200	No	

References

[1] a. J. J. E. Eerhart, a. P. C. Faaij, and M. K. Patel, "Replacing fossil based PET with biobased PEF; process analysis, energy and GHG balance," *Energy Environ. Sci.*, vol. 5, no. 4, p. 6407, 2012.

[2] E. De Jong, M. A. Dam, and L. Sipos, "Furandicarboxylic Acid (FDCA), A Versatile Building Block for a Very," pp. 1–13, 2012.

[3] S. K. Burgess, D. S. Mikkilineni, D. B. Yu, D. J. Kim, C. R. Mubarak, R. M. Kriegel, and W. J. Koros, "Water sorption in poly (ethylene furanoate) compared to poly (ethylene terephthalate). Part 2 : Kinetic sorption," *Polymer (Guildf).*, vol. 55, no. 26, pp. 6870–6882, 2014.

[4] S. K. Burgess, R. M. Kriegel, and W. J. Koros, "Oxygen sorption and transport in amorphous poly(ethylene furanoate)," *Macromolecules*, vol. 48, no. 7, pp. 2184–2193, 2015.

[5] S. K. Burgess, R. M. Kriegel, and W. J. Koros, "Carbon Dioxide Sorption and Transport in Amorphous Poly(ethylene furanoate)," 2015.

[6] S. K. Burgess, D. S. Mikkilineni, D. B. Yu, D. J. Kim, C. R. Mubarak, R. M. Kriegel, and W. J. Koros, "Water sorption in poly (ethylene furanoate) compared to poly (ethylene terephthalate). Part 2 : Kinetic sorption," *Polymer (Guildf).*, vol. 55, no. 26, pp. 6870–6882, 2014.

[7] S. K. Burgess, J. E. Leisen, B. E. Kraftschik, C. R. Mubarak, R. M. Kriegel, and W. J. Koros, "Chain Mobility, Thermal, and Mechanical Properties of Poly(ethylene furanoate) Compared to Poly(ethylene terephthalate)," 2014.

[8] V. A. Online, G. Z. Papageorgiou, V. Tsanaktsis, and D. N. Bikiaris, "polyester using monomers derived from renewable resources : thermal behavior comparison with PET and PEN †," pp. 7946–7958, 2014.

[9] T. Werpy and G. Petersen, "Top Value Added Chemicals from Biomass," *U.S. Dep. energy*, vol. 1, p. 76, 2004.

[10] G. G. Avantium and J. Avantium, "Furanics : Novel fuel options from carbohydrates," no. July, 2016.

[11] M. Bicker, J. Hirth, and H. Vogel, “Dehydration of fructose to 5-hydroxymethylfurfural in sub- and supercritical acetone,” *Green Chem.*, vol. 5, no. 2, pp. 280–284, 2003.

[12] H. Zhao, J. E. Holladay, H. Brown, and Z. C. Zhang, “Metal chlorides in ionic liquid solvents convert sugars to 5-hydroxymethylfurfural.,” *Science*, vol. 316, no. 5831, pp. 1597–1600, 2007.

[13] Y. Roman-Leshkov, “Phase Modifiers Promote Efficient Production of Hydroxymethylfurfural from Fructose,” *Science (80-.).*, vol. 312, no. 5782, pp. 1933–1937, 2006.

[14] R. J. Van Putten, J. C. Van Der Waal, E. De Jong, C. B. Rasrendra, H. J. Heeres, and J. G. De Vries, “Hydroxymethylfurfural, a versatile platform chemical made from renewable resources,” *Chemical Reviews*, vol. 113, no. 3. pp. 1499–1597, 2013.

[15] S. Siankevich, G. Savoglidis, Z. Fei, G. Laurenczy, D. T. L. Alexander, N. Yan, and P. J. Dyson, “A novel platinum nanocatalyst for the oxidation of 5-Hydroxymethylfurfural into 2,5-Furandicarboxylic acid under mild conditions,” *J. Catal.*, vol. 315, pp. 67–74, 2014.

[16] X. Tong, Y. Ma, and Y. Li, “Biomass into chemicals: Conversion of sugars to furan derivatives by catalytic processes,” *Appl. Catal. A Gen.*, vol. 385, no. 1–2, pp. 1–13, 2010.

[17] P. Gopalakrishnan, S. Narayan-Sarathy, T. Ghosh, K. Mahajan, and M. N. Belgacem, “Synthesis and characterization of bio-based furanic polyesters,” *J. Polym. Res.*, vol. 21, no. 1, 2014.

[18] A. Gandini and A. Silvestre, “The furan counterpart of poly (ethylene terephthalate): An alternative material based on renewable resources,” *J. Polym. ...*, vol. 5, no. c, pp. 295–298, 2009.

[19] “patent_PEFsynthesis_polycond.pdf.” .

[20] M. Jiang, Q. Liu, Q. Zhang, C. Ye, and G. Zhou, “A series of furan-aromatic polyesters synthesized via direct esterification method based on renewable resources,” *J. Polym. Sci. Part A Polym. Chem.*, vol. 50, no. 5, pp. 1026–1036, 2012.

[21] R. R. Burch, S. R. Lustig, and M. Spinu, “Synthesis of cyclic oligoesters and their rapid polymerization to high molecular weight,” *Macromolecules*, vol. 33, no. 14, pp. 5053–

5064, 2000.

[22] P. Hubbard, W. J. Brittain, W. J. Simonsick, and C. W. Ross, “Synthesis and Ring-Opening Polymerization of Poly(alkylene 2,6-naphthalenedicarboxylate) Cyclic Oligomers,” *Macromolecules*, vol. 29, no. 26, pp. 8304–8307, Jan. 1996.

[23] Odian G. (College of Staten Island), *Principles of polymerization*, no. 615. 1975.

[24] D. J. Brunelle, “Cyclic oligomer chemistry,” *J. Polym. Sci. Part A Polym. Chem.*, vol. 46, no. 4, pp. 1151–1164, 2008.

[25] B. G. G. Lohmeijer, R. C. Pratt, F. Leibfarth, J. W. Logan, D. A. Long, A. P. Dove, F. Nederberg, J. Choi, C. Wade, R. M. Waymouth, and J. L. Hedrick, “Guanidine and amidine organocatalysts for ring-opening polymerization of cyclic esters,” *Macromolecules*, vol. 39, no. 25, pp. 8574–8583, 2006.

[26] D. J. Brunelle and J. E. Bradt, “Method for preparation of macrocyclic poly(alkylene dicarboxylate) oligomers.pdf.”

[27] P. a Hubbard, W. J. Brittain, W. L. Mattice, and D. J. Brunelle, “Ring-Size Distribution in the Depolymerization of Poly(butylene Terephthalate),” *Society*, vol. 9297, no. 97, pp. 1518–1522, 1998.

[28] I. J. A. Mertens, L. W. Jenneskens, E. J. Vlietstra, A. C. van der Kerk-van Hoof, J. W. Zwikker, W. J. J. Smeets, and A. L. Spek, “Formation and isolation of huge cyclic oligomers: polycondensation of 1,5-bis(1-hydroxy-3,6,9-trioxanonyl)naphthalene and terephthaloyl chloride,” *J. Chem. Soc., Chem. Commun.*, vol. 2, no. 16, pp. 1621–1622, 1995.

[29] S. Thakur and S. N. Rao, *New Frontiers in Polymer Synthesis*, no. 1. Berlin, Heidelberg: Springer Berlin Heidelberg, 2008.

[30] M. a. Winnik, “Cyclization and the conformation of hydrocarbon chains,” *Chem. Rev.*, vol. 81, no. 5, pp. 491–524, 1981.

[31] S. Salhi, M. Tessier, R. El Gharbi, and A. Fradet, “Role of end-groups and catalyst in polyester cyclodepolymerization and cycle-chain equilibria,” *Polymer (Guildf).*, vol. 55, no. 1, pp. 73–82, Jan. 2014.

[32] A. Cingolani, P. Fleckenstein, and G. Storti, “Production of cyclic polyethylene furfural monomers for ring opening polymerization,” ETH, 2014.

[33] L. Ho Ting, P. Fleckenstein, and G. Storti, “Synthesis and Purification of Cyclic (Ethylene Furanoate) Oligomers Produced by Cyclodepolymerization,” ETH Zurich, 2015.

[34] J. C. Munoz Chen, P. Fleckenstein, and G. Storti, “Synthesis of Cyclic (Ethylene Furanoate) Oligomers via Reactive Distillation for Ring Opening Polymerization,” ETH Zurich.

[35] D. J. Brunelle, E. P. Boden, and T. G. Shannon, “Remarkably selective formation of macrocyclic aromatic carbonates: versatile new intermediates for the synthesis of aromatic polycarbonates,” *J. Am. Chem. Soc.*, vol. 112, no. 6, pp. 2399–2402, 1990.

[36] D. Pfister, G. Storti, F. Tancini, L. I. Costa, and M. Morbidelli, “Synthesis and Ring-Opening Polymerization of Cyclic Butylene 2 , 5-Furandicarboxylate,” *Macromol. Chem. Phys.*, vol. 216, no. 21, pp. 2141–2146, 2015.

[37] J. C. Morales-Huerta and A. Mart, “Sustainable Aromatic Copolyesters via Ring Opening Polymerization: Poly(butylene 2,5-furandicarboxylate- co -terephthalate)s,” *ACS Sustain. Chem.*, vol. 4, pp. 4965–4973, 2016.

[38] P. Hodge, “Entropically driven ring-opening polymerization of strainless organic macrocycles,” *Chem. Rev.*, vol. 114, no. 4, pp. 2278–2312, 2014.

[39] S. D. Kamau, P. Hodge, and M. Helliwell, “Cyclo-depolymerization of poly (propylene terephthalate): Some ring-opening polymerizations of the cyclic oligomers produced,” *Polym. Adv. Technol.*, vol. 14, no. 7, pp. 492–501, 2003.

[40] P. Hodge, “Cyclodepolymerization as a method for the synthesis of macrocyclic oligomers,” *React. Funct. Polym.*, vol. 80, no. 1, pp. 21–32, 2014.

[41] K. Sudesh and T. Iwata, “Sustainability of biobased and biodegradable plastics,” *Clean - Soil, Air, Water*, vol. 36, no. 5–6, pp. 433–442, 2008.

[42] F. Grün, H. Watanabe, Z. Zamanian, L. Maeda, K. Arima, R. Cubacha, D. M. Gardiner, J. Kanno, T. Iguchi, and B. Blumberg, “Endocrine-disrupting organotin compounds are potent inducers of adipogenesis in vertebrates.,” *Mol. Endocrinol.*, vol. 20, no. 9, pp. 2141–2155, 2006.

[43] T. Welton, “Solvents and sustainable chemistry Subject Areas : Author for correspondence :,” *R. Soc. Publ.*, vol. 471, 2015.

[44] P. Isnard, E. Guntrum, T. Senac, and P. Cruciani, “Sanofi’s Solvent Selection Guide: A Step Toward More Sustainable Processes,” *Am. Chem. Soc.*, vol. 17, pp. 1517–1525, 2013.

[45] A. D. Curzons, D. C. Constable, and V. L. Cunningham, “Solvent selection guide: a guide to the integration of environmental, health and safety criteria into the selection of solvents,” *Clean Prod. Process.*, vol. 1, no. 2, pp. 82–90, 1999.

[46] H. Jacobson and W. H. Stockmayer, “Intramolecular Reaction in Polycondensations. I. The Theory of Linear Systems,” *J. Chem. Phys.*, vol. 18, no. 12, pp. 1600–1606, 1950.

[47] Z.-R. Chen, J. P. Claverie, R. H. Grubbs, and J. a Kornfield, “Modeling ring-chain equilibria in ring-opening polymerization of cycloolefins,” *Macromolecules*, vol. 28, pp. 2147–2154, 1995.

[48] J. L. Webb and J. Mihalich, “Methods for preparation of macrocyclic polyesters oligomer via heterogeneous catalysis,” 2013.

[49] G. Bellussi, A. Carati, and R. Millini, *Industrial Potential of Zeolites*, vol. 2. 2010.

[50] S. W. Sohn, “Liquid Industrial Non - Aromatics Adsorptive Separations,” pp. 249–272, 2010.

[51] P. Cubillas and M. W. Anderson, *SynthesisMechanism: Crystal Growth and Nucleation*. 2010.

[52] J. V. Smith, “Definition of a zeolite,” *Zeolites*, vol. 4, no. 4, pp. 309–310, 1984.

[53] T. O. Drews and M. Tsapatsis, “Progress in manipulating zeolite morphology and related applications,” *Current Opinion in Colloid and Interface Science*, vol. 10, no. 5–6. pp. 233–238, 2005.

[54] L. B. Mccusker and C. Baerlocher, *Zeolites and Ordered Mesoporous Materials: Progress and Prospects*, vol. 157. Elsevier B.V., 2005.

[55] J. Yu, *Chapter 3 Synthesis of zeolites*, vol. 168. Elsevier B.V., 2007.

[56] W. J. Taylor, “Average Length and Radius of Normal Paraffln Hydrocarbon Molecules,” *J. Chem. Phys.*, vol. 16, no. 1948, p. 257, 1948.

[57] J. Flory, “Kinetics of Polyesterification : A Study of the Effects of Molecular Weight and Viscosity on Reaction Rate,” *J. Am. Chem. Soc.*, vol. 61, no. 12, pp. 3334–3340, 1939.

[58] H. K. Mitchell, E. E. Snell, and R. J. Williams, “Kinetics of the Degradation of Polyester by Alcohols,” *J. Am. Chem. Soc.*, vol. 62, no. 9, pp. 324–5, 1940.

[59] P. J. Flory, “Fundamental principles of condensation polymerization.,” *Chem. Rev.*, vol. 39, no. 1, pp. 137–197, 1946.

[60] F. Codari, “Poly (Lactic Acid) Polycondensation , Degradation and Nanoparticles synthesis,” 2011.

[61] S. W. v. d. Poll, “Cyclic Monomer Production for Renewable-Resource based Polymers (PEF) by Depolymerization.,” ETH Zurich, 2014.

[62] Z. Zhang, B. Liu, and Z. Zhao, “Conversion of fructose into 5-HMF catalyzed by GeCl 4 in DMSO and [Bmim]Cl system at room temperature,” *Carbohydr. Polym.*, vol. 88, no. 3, pp. 891–895, 2012.

[63] J. J. Bozell and G. R. Petersen, “Technology development for the production of biobased products from biorefinery carbohydrates—the US Department of Energy’s ‘Top 10’ revisited,” *Green Chem.*, vol. 12, no. 4, p. 539, 2010.

[64] P. J. Flory, “Foundations of Rotational Isomeric State Theory and General Methods for Generating Configurational Averages,” *Macromolecules*, vol. 7, no. 3, pp. 381–392, 1974.

[65] S. M. Auerbach, K. A. Carrado, and P. K. Dutta, *Handbook of Zeolite Science and Technology*. .

[66] D. E. De Vos and P. A. Jacobs, “Zeolite effects in liquid phase organic transformations,” in *Microporous and Mesoporous Materials*, 2005, vol. 82, no. 3, pp. 293–304.

[67] T. W. Lyons, D. Guironnet, M. Findlater, and M. Brookhart, “Synthesis of p-xylene from ethylene,” *J. Am. Chem. Soc.*, vol. 134, no. 38, pp. 15708–15711, 2012.